

Nonlinear k_{\perp} -factorization for Forward Dijets in DIS off Nuclei in the Saturation regime

N.N. Nikolaev^{a,b}, W. Schäfer^a, B.G. Zakharov^b, V.R. Zoller^c

^a) Institut f. Kernphysik, Forschungszentrum Jülich, D-52425 Jülich, Germany

^b) L.D.Landau Institute for Theoretical Physics, Chernogolovka, Russia

^c) Institute for Theoretical and Experimental Physics, Moscow, Russia

Abstract

We develop the QCD description of the breakup of photons into forward dijets in small- x deep inelastic scattering off nuclei in the saturation regime. Based on the color dipole approach, we derive a multiple scattering expansion for intranuclear distortions of the jet-jet transverse momentum spectrum. A special attention is paid to the non-Abelian aspects of the propagation of color dipoles in a nuclear medium. We report a nonlinear k_{\perp} -factorization formula for the breakup of photons into dijets in terms of the collective Weizsäcker-Williams (WW) glue of nuclei as defined in ref. [5, 6]. For hard dijets with the transverse momenta above the saturation scale the azimuthal decorrelation (acoplanarity) momentum is of the order of the nuclear saturation momentum Q_A . For minijets with the transverse momentum below the saturation scale the nonlinear k_{\perp} -factorization predicts a complete disappearance of the jet-jet correlation. We comment on a possible relevance of the nuclear decorrelation of jets to the experimental data from the STAR-RHIC Collaboration.

1 Introduction

From the parton model point of view the opacity of heavy nuclei to high energy projectiles entails a highly nonlinear relationship between the parton densities of free nucleons and nuclei. The trademark of the conventional pQCD factorization theorems for hard interactions of leptons and hadrons is that the hard scattering observables are linear functionals of the appropriate parton densities in the projectile and target [1]. The parton model interpretation of hard phenomena in ultrarelativistic heavy ion collisions calls upon the understanding of factorization properties in the nonlinear regime. A priori it is not obvious that one can define nuclear parton densities such that they enter different observables in a universal manner. Indeed, opacity of nuclei brings in a new large scale Q_A which separates the regimes of opaque nuclei and weak attenuation [2, 3, 4, 5]. Furthermore, for parton momenta below the saturation scale Q_A the evolution of sea from gluons was shown to be dominated by the anti-collinear, anti-DGLAP splitting [5]. In our early studies [5, 6] we have demonstrated that such observables as the amplitude of coherent hard diffractive breakup of a projectile on a nucleus or the transverse momentum distribution of forward quark and antiquark jets in deep inelastic scattering (DIS) off nucleus and/or the sea parton density of nuclei can be cast in precisely the same k_{\perp} -factorization form as for a free nucleon target. Specifically, one only needs to substitute the unintegrated gluon structure function (SF) of the free nucleon by the collective nuclear Weizsäcker-Williams (WW) unintegrated nuclear glue, which is an expansion over the collective gluon SF of spatially overlapping nucleons of the Lorentz-contracted ultrarelativistic nucleus. This exact correspondence between the BFKL unintegrated glue of the free nucleon [7] and nonlinear collective WW glue of the nucleus in the calculation of these observables is a heartening finding. It persists despite the the sea quarks and antiquarks with the transverse momenta below Q_A being generated by the anticollinear, anti-DGLAP splitting of gluons into sea, when the transverse momentum of the parent gluons is larger than the momentum of the produced sea quarks.

In [5] we noticed that less inclusive quantities like a spectrum of leading quarks from the truly inelastic DIS or coherent diffractive breakup off nuclei are nonlinear functionals of the collective nuclear WW glue. Consequently, in the quest for factorization properties of nuclear interactions one must go beyond the one-parton observables such as the amplitude of coherent diffractive breakup of pions or photons into dijets, single-jet inclusive cross section and/or nuclear sea parton density. In this communication we discuss truly inelastic hard interaction with nuclei followed by a breakup of the projectile into forward hard dijets ¹. We illustrate our major point on an example of DIS at small x with a breakup of the (virtual) photon into a hard approximately back-to-back dijet with small separation in rapidity, such that the so-called lightcone plus-components of the jet momenta sum up to the lightcone plus-component of the photon's momentum, i.e., the so-called $x_{\gamma} = 1$ criterion is fulfilled (e.g., see [10] and references therein). In

¹The preliminary results from this study have been reported elsewhere [8, 9]

the familiar collinear approximation such a dijet originates from the photon-gluon fusion $\gamma^*g \rightarrow q\bar{q}$, often referred to as an interaction of the unresolved or direct photon. The allowance for the transverse momentum of gluons leads to a disparity of the momenta and to an azimuthal decorrelation of the quark and antiquark jets which in DIS off free protons within the k_\perp -factorization can be quantified in terms of the unintegrated gluon SF of the target (see [11, 12] and references therein). A substantial nuclear broadening of the unintegrated gluon SF of nuclei at small x and of the nuclear sea parton distributions [5, 2] points at a stronger azimuthal decorrelation of jets produced in DIS off nuclei. Furthermore, our finding of anticollinear, anti-DGLAP splitting of gluons into sea suggests strongly a complete azimuthal decorrelation of forward quark and antiquark jets with the transverse momenta below the saturation scale, $p_\pm \lesssim Q_A$. In this communication we quantify these expectations and formulate a nonlinear generalization of the k_\perp -factorization for inclusive dijet spectrum.

The technical basis of our approach is the color-dipole multiple-scattering theory of small- x DIS off nuclei [13, 14]. We derive a consistent k_\perp -factorization description of the azimuthal decorrelation of jets in terms of the collective Weizsäcker-Williams unintegrated gluon SF of the nucleus. In this derivation we follow closely our early work [5] on the color-dipole approach to saturation of nuclear partons. We focus on DIS at $x \lesssim x_A = 1/R_A m_N \ll 1$ which is dominated by interactions of $q\bar{q}$ Fock states of the photon. Here m_N is the nucleon mass and R_A is the radius of the target nucleus of mass number A . Nuclear attenuation of these $q\bar{q}$ color dipoles [13, 15] quantifies the fusion of gluons and sea quarks from spatially overlapping nucleons of the Lorentz contracted nucleus ([16], see also [3, 4]). Here we report also some of the technical details, especially on the non-Abelian aspects of propagation of color dipoles in nuclear matter, which were omitted in the letter publication [5].

We focus on the genuinely inelastic DIS followed by color excitation of the target nucleus. For heavy nuclei of equal importance is coherent diffractive DIS in which the target nucleus does not break and is retained in the ground state. Coherent diffractive DIS makes 50 per cent of the total DIS events at small x [14], and in these coherent diffractive events quark and antiquark jets are produced exactly back-to-back with negligibly small transverse decorrelation momentum $|\Delta| = |\mathbf{p}_+ + \mathbf{p}_-| \lesssim 1/R_A \sim m_\pi/A^{1/3}$.

The further presentation is organized as follows. We work at the parton level and discuss the transverse momentum distribution of the final state quark and antiquark in interactions of $q\bar{q}$ Fock states of the photon with heavy nuclei. In section 2 we set up the formalism with a brief discussion of the decorrelation of jets in DIS off free nucleons. In section 3 we report a derivation of the general formula for the two-body transverse momentum distribution. Color exchange between the initially color-neutral $q\bar{q}$ dipole and nucleons of the target nucleus lead to an intranuclear propagation of the color-octet $q\bar{q}$ -states. Our formalism, based on the technique [17, 18], includes consistently the diffractive attenuation of color dipoles and effects of transitions between color-singlet and color-octet $q\bar{q}$ -pairs, as well as between different color states of the $q\bar{q}$ -pair. The hard jet-jet inclusive cross section is discussed in section 4. For hard dijets diffractive attenuation effects are weak and we obtain a nuclear k_\perp -factorization formula for the broadening of azimuthal correlations between the quark and antiquark jets, which is

reminiscent of that for a free nucleon target and is still a linear functional of the collective WW gluon SF of the nucleus. We relate the decorrelation (acoplanarity) momentum to the nuclear saturation scale Q_A . In section 5 working to large- N_c approximation we derive our central result - a nonlinear nuclear k_\perp -factorization formula for the inclusive dijet cross section and prove a complete disappearance of the jet-jet correlation for minijets with the transverse momentum below the saturation scale Q_A . In section 6 we present numerical estimates for the acoplanarity momentum distribution based on the unintegrated glue of the proton determined in [19]. We point out a strong enhancement of decorrelations from average to central DIS and comment on possible relevance of our mechanism of azimuthal decorrelations to the recent observation of the dissolution of the away jets in central nuclear collisions at RHIC [20]. The next-to-leading order $1/N_c^2$ corrections to the large- N_c results of section 5 are discussed in section 7. Here we derive the nonlinear k_\perp -factorization representation for the $\propto 1/N_c^2$ corrections and establish a close connection between the $1/N_c^2$ and higher-twist expansions. In the Conclusions section we summarize our principal findings.

Some of the technical details are presented in the Appendices. In Appendix A we present the calculation of the matrix of 4-body cross sections which enters the evolution operator for the intranuclear propagation of color dipoles. In Appendix B we revisit the single-jet spectrum and total cross section of DIS off nuclei and demonstrate how the color-dipole extension [13, 14] of the Glauber-Gribov results [21, 22] is recovered despite a nontrivial spectrum of eigen-cross sections for non-Abelian propagation of color dipoles in a nuclear matter. The properties of collective unintegrated gluon SF for overlapping nucleons of the Lorentz-contracted ultrarelativistic nucleus are discussed in Appendix C.

2 k_\perp -factorization for breakup of photons into forward dijets in DIS off free nucleons

We recall briefly the color dipole formulation of DIS [13, 14, 23, 24, 25] and set up a formalism on an example of jet-jet decorrelation in DIS off free nucleons which at moderately small x is dominated by interactions of $q\bar{q}$ states of the photon. The total cross section for interaction of the color dipole \mathbf{r} with the target nucleon equals [26, 27]

$$\begin{aligned}\sigma(r) &= \alpha_S(r)\sigma_0 \int d^2\boldsymbol{\kappa} f(\boldsymbol{\kappa}) [1 - \exp(i\boldsymbol{\kappa}\mathbf{r})] \\ &= \frac{1}{2}\alpha_S(r)\sigma_0 \int d^2\boldsymbol{\kappa} f(\boldsymbol{\kappa}) [1 - \exp(i\boldsymbol{\kappa}\mathbf{r})] \cdot [1 - \exp(-i\boldsymbol{\kappa}\mathbf{r})],\end{aligned}\quad (1)$$

where σ_0 is an auxiliary soft parameter, $f(\boldsymbol{\kappa})$ is normalized as $\int d^2\boldsymbol{\kappa} f(\boldsymbol{\kappa}) = 1$ and is related to the BFKL unintegrated gluon SF of the target nucleon ([7], for the phenomenology and review see [19, 28]) $\mathcal{F}(x, \kappa^2) = \partial G(x, \kappa^2)/\partial \log \kappa^2$ by

$$f(\boldsymbol{\kappa}) = \frac{4\pi}{N_c\sigma_0} \cdot \frac{1}{\kappa^4} \cdot \mathcal{F}(x, \kappa^2). \quad (2)$$

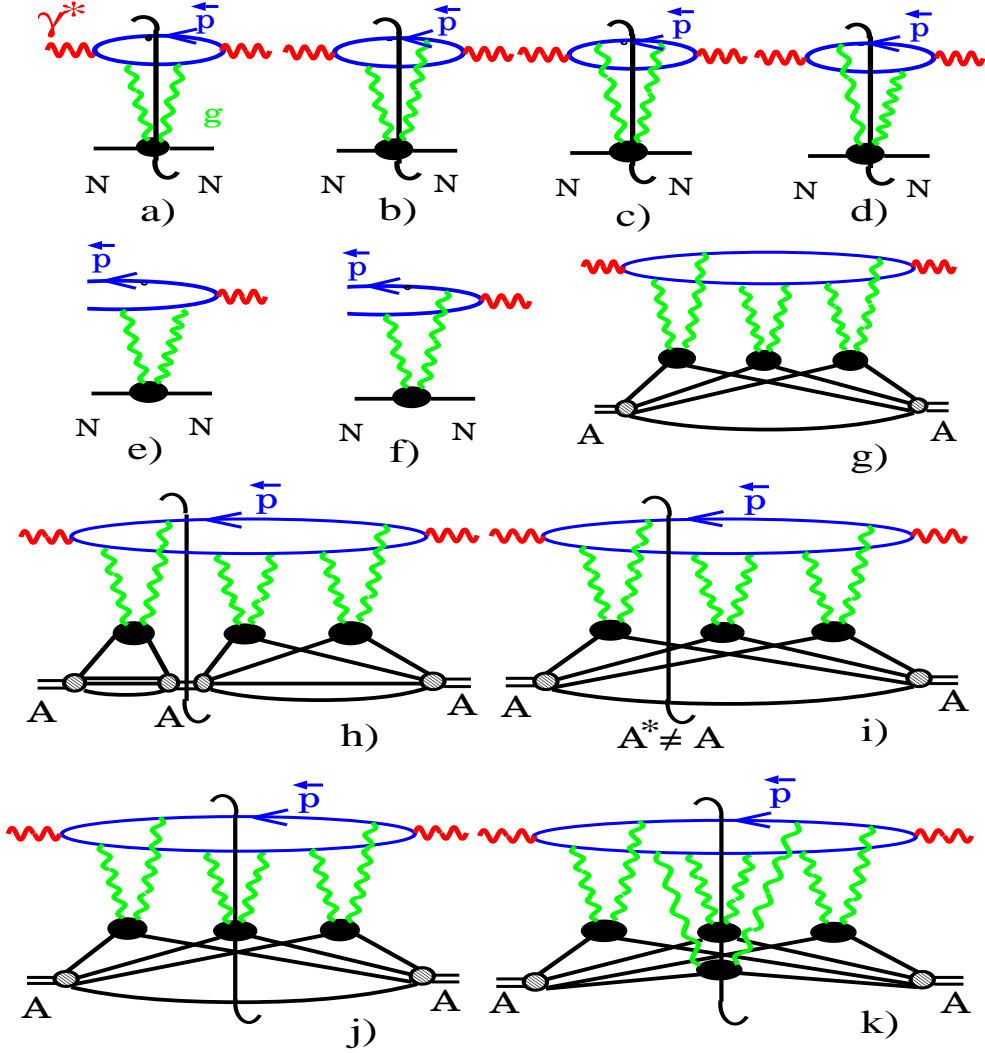


Figure 1: *The pQCD diagrams for cross section of inclusive DIS off nucleons (a-d) and nuclei (g-k) and the amplitude of diffractive DIS off protons (e,f). Diagrams (a-d) show the unitarity cuts with color excitation of the target nucleon, (g) - a generic multiple scattering diagram for the amplitude of Compton scattering off nucleus, (h) - the unitarity cut for a coherent diffractive DIS with retention of the ground state nucleus A in the final state, (i) - the unitarity cut for quasielastic diffractive DIS with excitation and breakup of the nucleus A^* , (j,k) - the unitarity cuts for truly inelastic DIS with single (j) and multiple (k) color excitation of nucleons of the nucleus.*

For DIS off a free nucleon target, see figs. 1a-1d, the total photoabsorption cross section equals [13]

$$\sigma_N(Q^2, x) = \int d^2\mathbf{r} dz |\Psi(Q^2, z, \mathbf{r})|^2 \sigma(x, \mathbf{r}), \quad (3)$$

where $\Psi(Q^2, z, \mathbf{r})$ is the wave function of the $q\bar{q}$ Fock state of the photon, Q^2 and x are

the standard DIS variables. In the momentum representation,

$$\frac{d\sigma_N}{d^2\mathbf{p}_+dz} = \frac{\sigma_0}{2} \cdot \frac{\alpha_S(\mathbf{p}_+^2)}{(2\pi)^2} \int d^2\boldsymbol{\kappa} f(\boldsymbol{\kappa}) |\langle\gamma^*|z, \mathbf{p}_+\rangle - \langle\gamma^*|z, \mathbf{p}_+ - \boldsymbol{\kappa}\rangle|^2, \quad (4)$$

where \mathbf{p}_+ is the transverse momentum of the quark, the antiquark has the transverse momentum $\mathbf{p}_- = -\mathbf{p}_+ + \boldsymbol{\kappa}$, and $z_+ = z$ and $z_- = 1 - z$ are the fractions of photon's lightcone momentum carried by the quark and antiquark, respectively. The variables z_{\pm} for the observed jets add up to unity, $x_\gamma = z_+ + z_- = 1$, which in the realm of DIS is referred to as the unresolved/direct photon interaction.

Upon summing over the helicities $\lambda, \bar{\lambda}$ of the final state quark and antiquark for transverse photons and flavor f we have

$$\begin{aligned} & |\langle\gamma^*|z, \mathbf{p}\rangle - \langle\gamma^*|z, \mathbf{p} - \boldsymbol{\kappa}\rangle|_{\lambda_\gamma=\pm 1}^2 = \\ & 2N_c e_f^2 \alpha_{em} \left\{ [z^2 + (1-z)^2] \left(\frac{\mathbf{p}}{\mathbf{p}^2 + \varepsilon^2} - \frac{\mathbf{p} - \boldsymbol{\kappa}}{(\mathbf{p} - \boldsymbol{\kappa})^2 + \varepsilon^2} \right)_{\lambda+\bar{\lambda}=0}^2 \right. \\ & \left. + m_f^2 \left(\frac{1}{\mathbf{p}^2 + \varepsilon^2} - \frac{1}{(\mathbf{p} - \boldsymbol{\kappa})^2 + \varepsilon^2} \right)_{\lambda+\bar{\lambda}=\lambda_\gamma}^2 \right\} \end{aligned} \quad (5)$$

and for longitudinal photons

$$\begin{aligned} & |\langle\gamma^*|z, \mathbf{p}\rangle - \langle\gamma^*|z, \mathbf{p} - \boldsymbol{\kappa}\rangle|_{\lambda_\gamma=0}^2 = \\ & 8N_c e_f^2 \alpha_{em} Q^2 z^2 (1-z)^2 \left(\frac{1}{\mathbf{p}^2 + \varepsilon^2} - \frac{1}{(\mathbf{p} - \boldsymbol{\kappa})^2 + \varepsilon^2} \right)_{\lambda+\bar{\lambda}=\lambda_\gamma}^2, \end{aligned} \quad (6)$$

where $\varepsilon^2 = z(1-z)Q^2 + m_f^2$.

Now, notice that the transverse momentum of the gluon is precisely the decorrelation momentum $\boldsymbol{\Delta} = \mathbf{p}_+ + \mathbf{p}_-$, so that in the still further differential from

$$\begin{aligned} \frac{d\sigma_N}{dzd^2\mathbf{p}_+d^2\boldsymbol{\Delta}} &= \frac{\sigma_0}{2} \cdot \frac{\alpha_S(\mathbf{p}^2)}{(2\pi)^2} f(\boldsymbol{\Delta}) |\langle\gamma^*|z, \mathbf{p}_+\rangle - \langle\gamma^*|z, \mathbf{p}_+ - \boldsymbol{\Delta}\rangle|^2 \\ &= \frac{\alpha_S(\mathbf{p}^2)}{2\pi N_c} \cdot \frac{\mathcal{F}(x, \boldsymbol{\Delta}^2)}{\Delta^4} \cdot |\langle\gamma^*|z, \mathbf{p}_+\rangle - \langle\gamma^*|z, \mathbf{p}_+ - \boldsymbol{\Delta}\rangle|^2. \end{aligned} \quad (7)$$

The small- x result (7) shows that in DIS forward dijets acquire their large transverse momentum from the intrinsic momentum of quark and antiquark in the wave function of the projectile photon, hence dubbing this process a breakup of the photon into forward hard dijets is appropriate. Besides the criterion $x_\gamma = 1$ the experimental signature of the photon breakup is a small rapidity separation of forward jets, i.e., $z_+ \sim z_-$. The perturbative hard scale for our process is set by $(4\mathbf{p}_+^2 + Q^2)$ and gluon SF of the proton enters (7) at the Bjorken variable $x = (4\mathbf{p}_+^2 + Q^2)/W^2$, where W is the γ^*p center of mass energy. The purpose of our study is an extension of (7) to breakup of photons into dijets in truly inelastic DIS on nuclear targets.

3 Breakup of photons into dijets on nuclear targets

We focus on DIS at $x \lesssim x_A = 1/R_A m_N \ll 1$ which is dominated by interactions of $q\bar{q}$ states of the photon. This is a starting term of the leading $\log \frac{1}{x}$ expansion, extension to interactions of higher Fock states of the photon and corresponding $\log \frac{1}{x}$ evolution to smaller x will be discussed elsewhere. For $x \lesssim x_A$ the propagation of the $q\bar{q}$ pair inside nucleus can be treated in the straight-path approximation.

We work in the conventional approximation of two t-channel gluons in DIS off free nucleons. The relevant unitarity cuts of the forward Compton scattering amplitude are shown in figs. 1a-1d and describe the transition from the color-neutral $q\bar{q}$ dipole to color-octet $q\bar{q}$ pair². The two-gluon exchange approximation amounts to neglecting unitarity constraints in DIS off free nucleons. As a quantitative measure of unitarity corrections one can take diffractive DIS off free nucleons the amplitude of which is described by higher order diagrams of fig. 1e,f [23, 24, 27] and which is only a small fraction of total DIS, $\eta_D \ll 1$ [29, 30, 31]. The unitarity cuts of the nuclear Compton scattering amplitude which correspond to the genuine inelastic DIS with color excitation of the nucleus are shown in figs. 1j,k. The diagram 1k describes a consecutive color excitation of the target nucleus accompanied by the color-space rotation of the color-octet $q\bar{q}$.

Let \mathbf{b}_+ and \mathbf{b}_- be the impact parameters of the quark and antiquark, respectively, and $S_A(\mathbf{b}_+, \mathbf{b}_-)$ be the S-matrix for interaction of the $q\bar{q}$ pair with the nucleus. We are interested in the truly inelastic inclusive cross section summed over all excitations of the target nucleus when one or several nucleons have been color excited. A convenient way to sum such cross sections is offered by the closure relation [21]. Regarding the color states c_{km} of the $q_k\bar{q}_m$ pair, we sum over all octet and singlet states. Then the 2-jet inclusive spectrum is calculated in terms of the 2-body density matrix as

$$\begin{aligned} \frac{d\sigma_{in}}{dzd^2\mathbf{p}_+d^2\mathbf{p}_-} &= \frac{1}{(2\pi)^4} \int d^2\mathbf{b}'_+ d^2\mathbf{b}'_- d^2\mathbf{b}_+ d^2\mathbf{b}_- \\ &\times \exp[-i\mathbf{p}_+(\mathbf{b}_+ - \mathbf{b}'_+) - i\mathbf{p}_-(\mathbf{b}_- - \mathbf{b}'_-)] \Psi^*(Q^2, z, \mathbf{b}'_+ - \mathbf{b}'_-) \Psi(Q^2, z, \mathbf{b}_+ - \mathbf{b}_-) \\ &\times \left\{ \sum_{A^*} \sum_{km} \langle 1; A | S_A^*(\mathbf{b}'_+, \mathbf{b}'_-) | A^*; c_{km} \rangle \langle c_{km}; A^* | S_A(\mathbf{b}_+, \mathbf{b}_-) | A; 1 \rangle \right. \\ &\left. - \langle 1; A | S_A^*(\mathbf{b}'_+, \mathbf{b}'_-) | A; 1 \rangle \langle 1; A | S_A(\mathbf{b}_+, \mathbf{b}_-) | A; 1 \rangle \right\}. \end{aligned} \quad (8)$$

In the integrand of (8) we subtracted the coherent diffractive component of the final state. Notice, that four straight-path trajectories $\mathbf{b}_\pm, \mathbf{b}'_\pm$ enter the calculation of the full fledged 2-body density matrix and S_A and S_A^* describe the propagation of two quark-antiquarks pairs, $q\bar{q}$ and $q'\bar{q}'$, inside a nucleus.

The further analysis of the integrand of (8) is a non-Abelian generalization of the formalism developed by one of the authors (BGZ) for the in-medium evolution of ultra-relativistic positronium [32]. Upon the application of closure to sum over nuclear final states A^* the integrand of (8) can be considered as an intranuclear evolution operator

²To be more precise, for arbitrary N_c color-excited $q\bar{q}$ pair is in the adjoint representation and quarks in fundamental representation of $SU(N_c)$, our reference to the color octet and triplet must not cause any confusion.

for the 2-body density matrix (for the related discussion see also ref. [33])

$$\begin{aligned} \sum_{A^*} \sum_{km} \langle A | \{ \langle 1 | S_A^*(\mathbf{b}'_+, \mathbf{b}'_-) | c_{km} \rangle \} | A^* \rangle \langle A^* | \{ \langle c_{km} | S_A(\mathbf{b}_+, \mathbf{b}_-) | 1 \rangle \} | A \rangle = \\ = \langle A | \left\{ \sum_{km} \langle 1 | S_A^*(\mathbf{b}'_+, \mathbf{b}'_-) | c_{km} \rangle \langle c_{km} | S_A(\mathbf{b}_+, \mathbf{b}_-) | 1 \rangle \right\} | A \rangle. \end{aligned} \quad (9)$$

Let the eikonal for the quark-nucleon and antiquark-nucleon QCD gluon exchange interaction be $T_+^a \chi(\mathbf{b})$ and $T_-^a \chi(\mathbf{b})$, where T_+^a and T_-^a are the $SU(N_c)$ generators for the quark and antiquarks states, respectively. The vertex V_a for excitation of the nucleon $g^a N \rightarrow N_a^*$ into color octet state is so normalized that after application of closure the vertex $g^a g^b NN$ in the diagrams of fig. 1a-d is δ_{ab} . Then, to the two-gluon exchange approximation, the S -matrix of the $(q\bar{q})$ -nucleon interaction equals

$$S_N(\mathbf{b}_+, \mathbf{b}_-) = 1 + i[T_+^a \chi(\mathbf{b}_+) + T_-^a \chi(\mathbf{b}_-)] V_a - \frac{1}{2} [T_+^a \chi(\mathbf{b}_+) + T_-^a \chi(\mathbf{b}_-)]^2. \quad (10)$$

The profile function for interaction of the $q\bar{q}$ dipole with a nucleon is $\Gamma(\mathbf{b}_+, \mathbf{b}_-) = 1 - S_N(\mathbf{b}_+, \mathbf{b}_-)$. For a color-singlet dipole $(T_+^a + T_-^a)^2 = 0$ and the dipole cross section for interaction of the color-singlet $q\bar{q}$ dipole with the nucleon equals

$$\sigma(\mathbf{b}_+ - \mathbf{b}_-) = 2 \int d^2 \mathbf{b}_+ \langle N | \Gamma(\mathbf{b}_+, \mathbf{b}_-) | N \rangle = \frac{N_c^2 - 1}{2N_c} \int d^2 \mathbf{b}_+ [\chi(\mathbf{b}_+) - \chi(\mathbf{b}_-)]^2. \quad (11)$$

The nuclear S -matrix of the straight-path approximation is

$$S_A(\mathbf{b}_+, \mathbf{b}_-) = \prod_{j=1}^A S_N(\mathbf{b}_+ - \mathbf{b}_j, \mathbf{b}_- - \mathbf{b}_j),$$

where the ordering along the longitudinal path is understood. We evaluate the nuclear expectation value in (9) in the standard dilute gas approximation. To the two-gluon exchange approximation, per each and every nucleon N_j only the terms quadratic in $\chi(\mathbf{b}_j)$ must be kept in the evaluation of the single-nucleon matrix element

$$\langle N_j | S_N^*(\mathbf{b}'_+ - \mathbf{b}_j, \mathbf{b}'_- - \mathbf{b}_j) S_N(\mathbf{b}_+ - \mathbf{b}_j, \mathbf{b}_- - \mathbf{b}_j) | N_j \rangle$$

which enters the calculation of $S_A^* S_A$. Following the technique developed in [17, 18] we can reduce the calculation of the evolution operator for the 2-body density matrix (9) to the evaluation of the S -matrix $S_{4A}(\mathbf{b}_+, \mathbf{b}_-, \mathbf{b}'_+, \mathbf{b}'_-)$ for the scattering of a fictitious 4-parton state composed of the two quark-antiquark pairs in the overall color-singlet state. Because $(T_+^a)^* = -T_-^a$, within the two-gluon exchange approximation the quarks entering the complex-conjugate S_A^* in (9) can be viewed as antiquarks, so that

$$\begin{aligned} \sum_{km} \langle 1 | S_A^*(\mathbf{b}'_+, \mathbf{b}'_-) | c_{km} \rangle \langle c_{km} | S_A(\mathbf{b}_+, \mathbf{b}_-) | 1 \rangle \\ = \sum_{kmjl} \delta_{kl} \delta_{mj} \langle c_{km} c_{jl} | S_{4A}(\mathbf{b}'_+, \mathbf{b}'_-, \mathbf{b}_+, \mathbf{b}_-) | 11 \rangle, \end{aligned} \quad (12)$$

where $S_{4A}(\mathbf{b}'_+, \mathbf{b}'_-, \mathbf{b}_+, \mathbf{b}_-)$ is an S-matrix for the propagation of the two quark-antiquark pairs in the overall singlet state. While the first $q\bar{q}$ pair is formed by the initial quark q and antiquark \bar{q} at impact parameters \mathbf{b}_+ and \mathbf{b}_- , respectively, in the second $q'\bar{q}'$ pair the quark q' propagates at an impact parameter \mathbf{b}'_- and the antiquark \bar{q}' at an impact parameter \mathbf{b}'_+ . In the initial state both quark-antiquark pairs are in color-singlet states: $|in\rangle = |11\rangle$.

Let us introduce the normalized singlet-singlet and octet-octet states

$$|11\rangle = \frac{1}{N_c}(\bar{q}q)(\bar{q}'q'), \quad |88\rangle = \frac{2}{\sqrt{N_c^2 - 1}}(\bar{q}T^a q)(\bar{q}'T^a q'), \quad (13)$$

where N_c is the number of colors and T^a are the generators of $SU(N_c)$. Making use of the color Fiertz identity,

$$\delta_j^k \delta_l^m = \frac{1}{N_c} \delta_l^k \delta_j^m + 2 \sum_a (T^a)_l^k (T^a)_j^m, \quad (14)$$

the sum (12) over color states of the produced quark-antiquark pair can be represented as

$$\begin{aligned} \sum_{km} \langle C_{km} C_{km} | S_{4A}(\mathbf{b}'_+, \mathbf{b}'_-, \mathbf{b}_+, \mathbf{b}_-) | 11 \rangle &= \langle 11 | S_{4A}(\mathbf{b}'_+, \mathbf{b}'_-, \mathbf{b}_+, \mathbf{b}_-) | 11 \rangle \\ &+ \sqrt{N_c^2 - 1} \langle 88 | S_{4A}(\mathbf{b}'_+, \mathbf{b}'_-, \mathbf{b}_+, \mathbf{b}_-) | 11 \rangle. \end{aligned} \quad (15)$$

If $\sigma_4(\mathbf{b}'_+, \mathbf{b}'_-, \mathbf{b}_+, \mathbf{b}_-)$ is the color-dipole cross section operator for the 4-body state, then the evaluation of the nuclear expectation value for a dilute gas nucleus in the standard approximation of neglecting the size of color dipoles compared to a radius of heavy nucleus gives [21]

$$S_{4A}(\mathbf{b}'_+, \mathbf{b}'_-, \mathbf{b}_+, \mathbf{b}_-) = \exp\left\{-\frac{1}{2}\sigma_4(\mathbf{b}'_+, \mathbf{b}'_-, \mathbf{b}_+, \mathbf{b}_-)T(\mathbf{b})\right\}, \quad (16)$$

where $T(\mathbf{b}) = \int db_z n_A(b_z, \mathbf{b})$ is the optical thickness of a nucleus at an impact parameter $\mathbf{b} = \frac{1}{4}(\mathbf{b}_+ + \mathbf{b}'_+ + \mathbf{b}_- + \mathbf{b}'_-)$, (one should not confuse \mathbf{b} with the center of gravity of color dipoles where the impact parameters \mathbf{b}_\pm and \mathbf{b}'_\pm must be weighted with z_\pm , the difference between the two quantities is irrelevant here) and $n_A(b_z, \mathbf{b})$ is nuclear matter density with the normalization $\int d^2\mathbf{b} T(\mathbf{b}) = A$. The single-nucleon S-matrix (10) contains transitions from the color-singlet to the both color-singlet and color-octet $q\bar{q}$ pairs. However, only color-singlet operators contribute to $\langle N_j | S_N^*(\mathbf{b}'_+ - \mathbf{b}_j, \mathbf{b}'_- - \mathbf{b}_j) S_N(\mathbf{b}_+ - \mathbf{b}_j, \mathbf{b}_- - \mathbf{b}_j) | N_j \rangle$, and hence the matrix $\sigma_4(\mathbf{b}'_+, \mathbf{b}'_-, \mathbf{b}_+, \mathbf{b}_-)$ only includes transitions between the $|11\rangle$ and $|88\rangle$ color-singlet 4-parton states, the $|18\rangle$ states are not allowed.

The pQCD diagrams for the 4-body cross section are shown in fig.2. It is convenient to introduce

$$\mathbf{s} = \mathbf{b}_+ - \mathbf{b}'_+, \quad (17)$$

for the variable conjugate to the decorrelation momentum, and $\mathbf{r} = \mathbf{b}_+ - \mathbf{b}_-$, $\mathbf{r}' = \mathbf{b}'_+ - \mathbf{b}'_-$, in terms of which

$$\mathbf{b}_+ - \mathbf{b}'_- = \mathbf{s} + \mathbf{r}', \quad \mathbf{b}_- - \mathbf{b}'_+ = \mathbf{s} - \mathbf{r}, \quad \mathbf{b}_- - \mathbf{b}'_- = \mathbf{s} - \mathbf{r} + \mathbf{r}'. \quad (18)$$

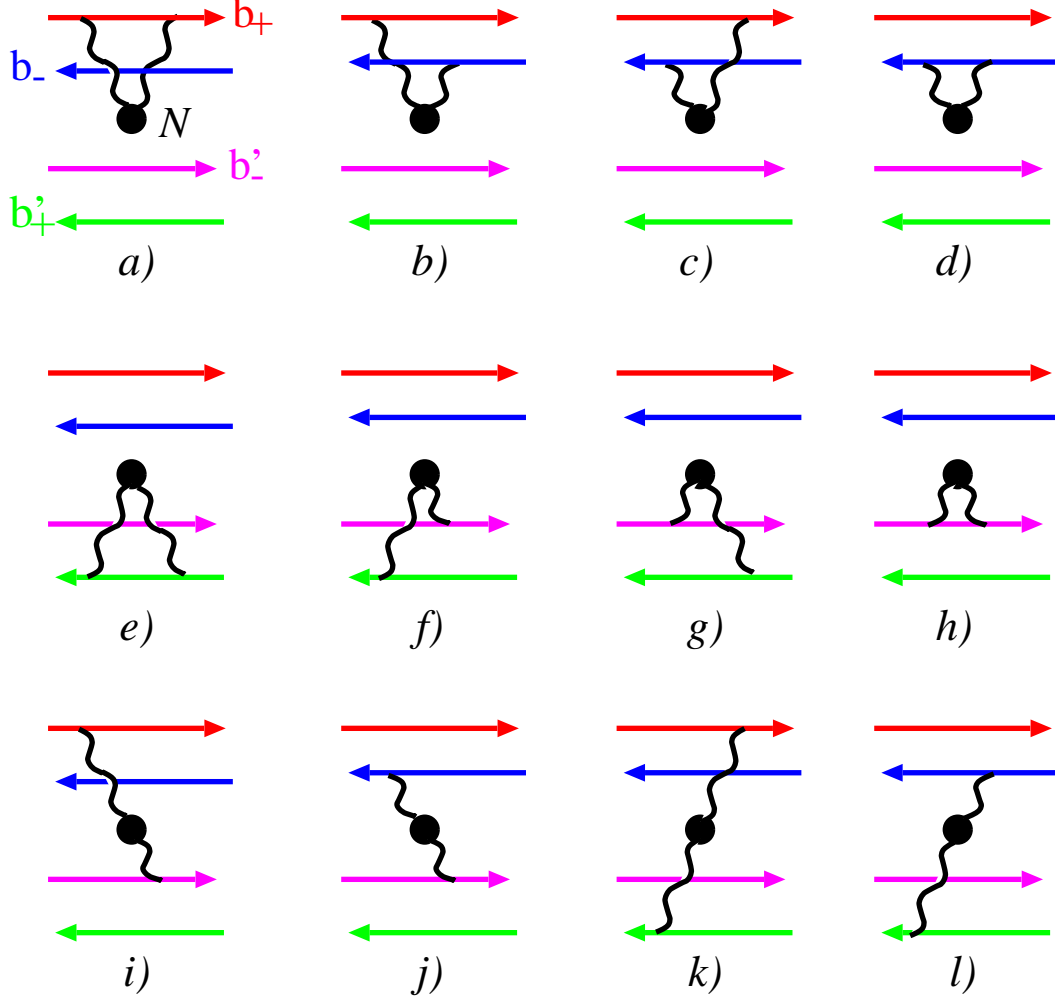


Figure 2: The pQCD diagrams for the matrix of color dipole cross section for the 4-body $(q\bar{q})(q'\bar{q}')$ state. The sets 4a-4d and 4e-4h show the diagrams for the scattering without changing the color state of the $q\bar{q}$ and $q'\bar{q}'$ dipoles, the set 4i-4l shows only half of the diagrams for scattering with rotation of the color state of dipoles.

Performing the relevant color algebra, we find (some details of the derivation are presented in Appendix A)

$$\sigma_{11} = \langle 11|\sigma_4|11\rangle = \sigma(\mathbf{r}) + \sigma(\mathbf{r}'), \quad (19)$$

$$\begin{aligned} \sigma_{18} = \langle 11|\sigma_4|88\rangle &= \frac{\sigma(\mathbf{s}) + \sigma(\mathbf{s} - \mathbf{r} + \mathbf{r}') - \sigma(\mathbf{s} + \mathbf{r}') - \sigma(\mathbf{s} - \mathbf{r})}{\sqrt{N_c^2 - 1}} \\ &= -\frac{\Sigma_{18}(\mathbf{s}, \mathbf{r}, \mathbf{r}')}{\sqrt{N_c^2 - 1}}, \end{aligned} \quad (20)$$

$$\sigma_{88} = \langle 88|\sigma_4|88\rangle = \frac{N_c^2 - 2}{N_c^2 - 1} [\sigma(\mathbf{s}) + \sigma(\mathbf{s} - \mathbf{r} + \mathbf{r}')]$$

$$+\frac{2}{N_c^2-1}[\sigma(\mathbf{s}+\mathbf{r}')+\sigma(\mathbf{s}-\mathbf{r})]-\frac{1}{N_c^2-1}[\sigma(\mathbf{r})+\sigma(\mathbf{r}')]. \quad (21)$$

The term in (8), which subtracts the contribution from diffractive processes without color excitation of the target nucleus, equals

$$\begin{aligned} &\langle 1; A|S_A^*(\mathbf{b}'_+, \mathbf{b}'_-)|A; 1\rangle \langle 1; A|S_A(\mathbf{b}_+, \mathbf{b}_-)|A; 1\rangle \\ &= \exp\left\{-\frac{1}{2}[\sigma(\mathbf{r})+\sigma(\mathbf{r}')T(\mathbf{b})]\right\} = \exp\left\{-\frac{1}{2}\sigma_{11}T(\mathbf{b})\right\}. \end{aligned} \quad (22)$$

In the discussion of nuclear effects it is convenient to use the Sylvester expansion

$$\exp\left\{-\frac{1}{2}\sigma_4 T(\mathbf{b})\right\} = \exp\left\{-\frac{1}{2}\Sigma_1 T(\mathbf{b})\right\} \frac{\sigma_4 - \Sigma_2}{\Sigma_1 - \Sigma_2} + \exp\left\{-\frac{1}{2}\Sigma_2 T(\mathbf{b})\right\} \frac{\sigma_4 - \Sigma_1}{\Sigma_2 - \Sigma_1}, \quad (23)$$

where $\Sigma_{1,2}$ are the two eigenvalues of the operator σ_4 ,

$$\Sigma_{1,2} = \frac{1}{2}(\sigma_{11} + \sigma_{88}) \mp \frac{1}{2}(\sigma_{11} - \sigma_{88}) \sqrt{1 + \frac{4\sigma_{18}^2}{(\sigma_{11} - \sigma_{88})^2}}. \quad (24)$$

An application to (15) of the Sylvester expansion gives for the integrand of (8)

$$\begin{aligned} &\sum_{A^*} \sum_{km} \langle 1; A|S_A^*(\mathbf{b}'_+, \mathbf{b}'_-)|A^*; c_{km}\rangle \langle c_{km}; A^*|S_A(\mathbf{b}_+, \mathbf{b}_-)|A; 1\rangle \\ &- \langle 1; A|S_A^*(\mathbf{b}'_+, \mathbf{b}'_-)|A; 1\rangle \langle 1; A|S_A(\mathbf{b}_+, \mathbf{b}_-)|A; 1\rangle \\ &= (\langle 11| + \sqrt{N_c^2-1}\langle 88|) \exp\left\{-\frac{1}{2}\sigma_4 T(\mathbf{b})\right\} |11\rangle - \exp\left\{-\frac{1}{2}\sigma_{11}T(\mathbf{b})\right\} \\ &= \exp\left\{-\frac{1}{2}\Sigma_2 T(\mathbf{b})\right\} - \exp\left\{-\frac{1}{2}\sigma_{11}T(\mathbf{b})\right\} \\ &+ \frac{\sigma_{11} - \Sigma_2}{\Sigma_1 - \Sigma_2} \left\{ \exp\left[-\frac{1}{2}\Sigma_1 T(\mathbf{b})\right] - \exp\left[-\frac{1}{2}\Sigma_2 T(\mathbf{b})\right] \right\} \\ &+ \frac{\sqrt{N_c^2-1}\sigma_{18}}{\Sigma_1 - \Sigma_2} \left\{ \exp\left[-\frac{1}{2}\Sigma_1 T(\mathbf{b})\right] - \exp\left[-\frac{1}{2}\Sigma_2 T(\mathbf{b})\right] \right\}. \end{aligned} \quad (25)$$

4 Breaking of photons into hard dijets: a still linear nuclear k_{\perp} -factorization

The diagonalization of the 2×2 matrix σ_4 is a straightforward task, so that technically eqs. (8) and (25) allow a direct calculation of the jet-jet inclusive cross section in terms of the color dipole cross section $\sigma(\mathbf{r})$. The evaluation of the 6-fold Fourier transform is not a trivial task, though.

First, notice that the difference between Σ_2 and $\sigma_{11} = \sigma(\mathbf{r}) + \sigma(\mathbf{r}')$ is quadratic or higher order in the off-diagonal σ_{18} , see eq. (24). Consequently, the first two lines in the Sylvester expansion (25) start with terms $\propto \sigma_{18}^2$, whereas the last line starts with terms

$\propto \sigma_{18}$. Then it is convenient to represent (25) as the impulse approximation (IA) term times the nuclear distortion factor $D_A(\mathbf{s}, \mathbf{r}, \mathbf{r}', \mathbf{b})$,

$$\begin{aligned}
& \sum_{A^*} \sum_{km} \langle 1; A | S_A^*(\mathbf{b}'_+, \mathbf{b}'_-) | A^*; c_{km} \rangle \langle c_{km}; A^* | S_A(\mathbf{b}_+, \mathbf{b}_-) | A; 1 \rangle \\
& - \langle 1; A | S_A^*(\mathbf{b}'_+, \mathbf{b}'_-) | A; 1 \rangle \langle 1; A | S_A(\mathbf{b}_+, \mathbf{b}_-) | A; 1 \rangle \\
& = T(\mathbf{b}) \Sigma_{18}(\mathbf{s}, \mathbf{r}, \mathbf{r}') D_A(\mathbf{s}, \mathbf{r}, \mathbf{r}', \mathbf{b}), \tag{26}
\end{aligned}$$

so that

$$\begin{aligned}
\frac{d\sigma_{in}}{d^2\mathbf{b} dz d^2\mathbf{p}_+ d^2\mathbf{p}_-} &= \frac{1}{2(2\pi)^4} \int d^2\mathbf{s} d^2\mathbf{r} d^2\mathbf{r}' \exp[-i(\mathbf{p}_+ + \mathbf{p}_-)\mathbf{s} + i\mathbf{p}_-(\mathbf{r}' - \mathbf{r})] \\
&\times \Psi^*(Q^2, z, \mathbf{r}') \Psi(Q^2, z, \mathbf{r}) T(\mathbf{b}) \Sigma_{18}(\mathbf{s}, \mathbf{r}, \mathbf{r}') D_A(\mathbf{s}, \mathbf{r}, \mathbf{r}', \mathbf{b}). \tag{27}
\end{aligned}$$

As an introduction to nuclear k_\perp -factorization, we start with forward hard jets with the momenta $\mathbf{p}_\pm^2 \gtrsim Q_A^2$, which are produced from interactions with the target nucleus of small color dipoles in the incident photon such that diffractive nuclear attenuation effects can be neglected. We proceed with the formulation of the Fourier representations for each factor in (26). The application of the integral representation (1) gives :

$$\begin{aligned}
\Sigma_{18}(\mathbf{s}, \mathbf{r}, \mathbf{r}') &= [\sigma(\mathbf{s}) - \sigma(\mathbf{s} + \mathbf{r}') - \sigma(\mathbf{s} - \mathbf{r}) + \sigma(\mathbf{s} - \mathbf{r} + \mathbf{r}')] \\
&= \alpha_S \sigma_0 \int d^2\boldsymbol{\kappa} f(\boldsymbol{\kappa}) \exp[i\boldsymbol{\kappa}\mathbf{s}] \{1 - \exp[i\boldsymbol{\kappa}\mathbf{r}']\} \{1 - \exp[-i\boldsymbol{\kappa}\mathbf{r}]\}. \tag{28}
\end{aligned}$$

Hard jets correspond to $|\mathbf{r}|, |\mathbf{r}'| \ll |\mathbf{s}|$. Then the two eigenvalues are $\Sigma_2 \approx \sigma_{11}$ and $\Sigma_1 \approx \sigma_{88} \approx 2\lambda_c \sigma(\mathbf{s})$, where $\lambda_c = N_c^2 / (N_c^2 - 1) = C_A / 2C_F$, where C_F and C_A are the Casimir operators for the fundamental and adjoint representations of $SU(N_c)$. Because of $\Sigma_2 \approx \sigma_{11} \approx 0$ only the last term, $\propto \sigma_{18}$, must be kept in the Sylvester expansion (25), and the nuclear distortion factor takes on a simple form

$$\begin{aligned}
D_A(\mathbf{s}, \mathbf{r}, \mathbf{r}', \mathbf{b}) &= \frac{2}{(\Sigma_2 - \Sigma_1)T(\mathbf{b})} \left\{ \exp\left[-\frac{1}{2}\Sigma_1 T(\mathbf{b})\right] - \exp\left[-\frac{1}{2}\Sigma_2 T(\mathbf{b})\right] \right\} \\
&= \frac{1 - \exp\left[-\frac{1}{2}\Sigma_1 T(\mathbf{b})\right]}{\frac{1}{2}\Sigma_1 T(\mathbf{b})}. \tag{29}
\end{aligned}$$

The Fourier representation for the nuclear distortion factor $D_A(\mathbf{s}, \mathbf{r}, \mathbf{r}')$ is readily obtained making use of the NSS representation for the nuclear attenuation factor [5, 6]

$$\begin{aligned}
\exp\left[-\frac{1}{2}\sigma(\mathbf{s})T(\mathbf{b})\right] &= \exp[-\nu_A(\mathbf{b})] \exp\left[\nu_A(\mathbf{b}) \int d^2\boldsymbol{\kappa} f(\boldsymbol{\kappa}) \exp(i\boldsymbol{\kappa}\mathbf{s})\right] \\
&= \exp[-\nu_A(\mathbf{b})] \sum_{j=0}^{\infty} \frac{\nu_A^j(\mathbf{b})}{j!} \int d^2\boldsymbol{\kappa} f^{(j)}(\boldsymbol{\kappa}) \exp(i\boldsymbol{\kappa}\mathbf{s}) \\
&= \int d^2\boldsymbol{\kappa} \Phi(\nu_A(\mathbf{b}), \boldsymbol{\kappa}) \exp(i\boldsymbol{\kappa}\mathbf{s}). \tag{30}
\end{aligned}$$

in terms of the nuclear Weizsäcker-Williams glue per unit area in the impact parameter plane, $\phi_{WW}(\nu_A(\mathbf{b}), \boldsymbol{\kappa})$, as defined in [5],

$$\Phi(\nu_A(\mathbf{b}), \boldsymbol{\kappa}) = \sum_{j=0}^{\infty} w_j(\nu_A(\mathbf{b})) f^{(j)}(\boldsymbol{\kappa}) = \exp(-\nu_A(\mathbf{b})) f^{(0)}(\boldsymbol{\kappa}) + \phi_{WW}(\nu_A(\mathbf{b}), \boldsymbol{\kappa}). \tag{31}$$

Here

$$\nu_A(\mathbf{b}) = \frac{1}{2}\alpha_S(r)\sigma_0 T(\mathbf{b}) \quad (32)$$

and

$$w_j(\nu_A(\mathbf{b})) = \frac{\nu_A^j(\mathbf{b})}{j!} \exp[-\nu_A(\mathbf{b})] \quad (33)$$

is a probability of finding j spatially overlapping nucleons in a Lorentz-contracted nucleus,

$$f^{(j)}(\boldsymbol{\kappa}) = \int \prod_{i=1}^j d^2\boldsymbol{\kappa}_i f(\boldsymbol{\kappa}_i) \delta(\boldsymbol{\kappa} - \sum_{i=1}^j \boldsymbol{\kappa}_i), \quad f^{(0)}(\boldsymbol{\kappa}) = \delta(\boldsymbol{\kappa}) \quad (34)$$

is a collective gluon field of j overlapping nucleons. As usual, the strong coupling in (32) must be taken at the hardest relevant scale [34].

The denominator Σ_1 in (29) is problematic from the point of view of the Fourier transform but can be eliminated by the integral representation

$$D_A(\mathbf{s}) = \int_0^1 d\beta \exp\left[-\frac{1}{2}\beta\Sigma_1 T(\mathbf{b})\right] = \int_0^1 d\beta \int d^2\boldsymbol{\kappa} \Phi(2\beta\lambda_c\nu_A(\mathbf{b}), \boldsymbol{\kappa}) \exp(i\boldsymbol{\kappa}\mathbf{s}). \quad (35)$$

Here β has a meaning of the fraction of the nuclear thickness which the $(q\bar{q})$ pair propagates in the color octet state. The introduction of this distortion factor into (27) is straightforward and gives our central result for the hard jet-jet inclusive cross section:

$$\frac{d\sigma_{in}}{d^2\mathbf{b}dzd^2\mathbf{p}_+d^2\boldsymbol{\Delta}} = T(\mathbf{b}) \int d^2\boldsymbol{\kappa} \int_0^1 d\beta \Phi(2\beta\lambda_c\nu_A(\mathbf{b}), \boldsymbol{\Delta} - \boldsymbol{\kappa}) \frac{d\sigma_N}{dzd^2\mathbf{p}_+d^2\boldsymbol{\kappa}}. \quad (36)$$

Since for hard jets $\mathbf{r}^2 \sim 1/\mathbf{p}_+^2$, one must use $\alpha_S(\mathbf{p}_+^2)$ in the evaluation of $\nu_A(\mathbf{b})$. For a thin nucleus such that $\nu_A(\mathbf{b}) \ll 1$, we have $\Phi(2\beta\lambda_c\nu_A(\mathbf{b}), \boldsymbol{\Delta} - \boldsymbol{\kappa}) = \delta(\boldsymbol{\Delta} - \boldsymbol{\kappa})$, see eq. (31), and recover the IA result

$$\frac{d\sigma_{in}}{d^2\mathbf{b}dzd^2\mathbf{p}_+d^2\boldsymbol{\Delta}} = T(\mathbf{b}) \frac{d\sigma_N}{dzd^2\mathbf{p}_+d^2\boldsymbol{\Delta}}. \quad (37)$$

Our result (36) for nuclear broadening of the acoplanarity momentum distribution of hard dijets can be regarded as a nuclear counterpart of the k_\perp -factorization result (7) for the free nucleon target.

The probabilistic form of a convolution eq. (36) of the differential cross section on a free nucleon target with the manifestly positive defined distribution $\Phi(2\beta\lambda_c\nu_A(\mathbf{b}), \boldsymbol{\kappa})$ can be understood as follows. Hard jets originate from small color dipoles. Their interaction with gluons of the target nucleus is suppressed by the mutual neutralization of color charges of the quark and antiquark in the small-sized color-singlet $q\bar{q}$ state which is manifest from the small cross section for a free nucleon target, see eq. (7). The first inelastic interaction inside a nucleus converts the $q\bar{q}$ pair into the color-octet state, in which color charges of the quark and antiquark do not neutralize each other, rescatterings of the quark and antiquark in the collective color field of intranuclear nucleons become uncorrelated, and the broadening of the momentum distribution with nuclear thickness follows a probabilistic picture.

5 Nonlinear nuclear k_{\perp} -factorization for breakup of photons into semihard dijets: large- N_c approximation

Now we are in the position to relax the hardness restriction and consider the semihard dijets, $|\mathbf{p}_{\pm}| \sim Q_A$. In this section we give a consistent treatment of this case in the venerable large- N_c approximation. What we shall formulate can be dubbed the nonlinear nuclear generalization of the k_{\perp} -factorization.

The crucial point is that in the large- N_c approximation $\Sigma_2 = \sigma_{11} = \sigma(\mathbf{r}) + \sigma(\mathbf{r}')$, so that only the last term in the Sylvester expansion (25) contributes to the jet-jet inclusive cross section. The nuclear distortion factor will be still given by eq. (29) but for finite Σ_2 . Upon the slight generalization of (35) and making use of

$$\Sigma_1 = \sigma(\mathbf{s}) + \sigma(\mathbf{s} + \mathbf{r}' - \mathbf{r}) \quad (38)$$

the distortion factor can be cast in the form

$$\begin{aligned} D_A(\mathbf{s}, \mathbf{r}, \mathbf{r}', \mathbf{b}) &= \int_0^1 d\beta \exp \left\{ -\frac{1}{2} [\beta \Sigma_1 + (1 - \beta) \Sigma_2] T(\mathbf{b}) \right\} \\ &= \int_0^1 d\beta \exp \left\{ -\frac{1}{2} (1 - \beta) [\sigma(\mathbf{r}) + \sigma(\mathbf{r}')] T(\mathbf{b}) \right\} \\ &\times \exp \left\{ -\frac{1}{2} \beta [\sigma(\mathbf{s}) + \sigma(\mathbf{s} + \mathbf{r}' - \mathbf{r})] T(\mathbf{b}) \right\} \end{aligned} \quad (39)$$

the different exponential factors in which admit a simple interpretation: The former two exponential factors describe the intranuclear distortion of the incoming color-singlet $(q\bar{q}) \& (q'\bar{q}')$ dipole state, whereas the last two factors describe the distortion of the outgoing color-octet $(q\bar{q}) \& (q'\bar{q}')$ states. Application of the NSS representation to attenuation factors in (39) yields

$$\begin{aligned} D_A(\mathbf{s}, \mathbf{r}, \mathbf{r}', \mathbf{b}) &= \int_0^1 d\beta \int d^2 \boldsymbol{\kappa}_1 \Phi((1 - \beta) \nu_A(\mathbf{b}), \boldsymbol{\kappa}_1) \exp(-i \boldsymbol{\kappa}_1 \mathbf{r}) \\ &\times \int d^2 \boldsymbol{\kappa}_2 \Phi((1 - \beta) \nu_A(\mathbf{b}), \boldsymbol{\kappa}_2) \exp(i \boldsymbol{\kappa}_2 \mathbf{r}) \\ &\times \int d^2 \boldsymbol{\kappa}_3 \Phi(\beta \nu_A(\mathbf{b}), \boldsymbol{\kappa}_3) \exp[i \boldsymbol{\kappa}_3 (\mathbf{s} + \mathbf{r}' - \mathbf{r})] \\ &\times \int d^2 \boldsymbol{\kappa}_4 \Phi(\beta \nu_A(\mathbf{b}), \boldsymbol{\kappa}_4) \exp(i \boldsymbol{\kappa}_4 \mathbf{r}) \end{aligned} \quad (40)$$

The integral representation (39) furnishes two important tasks: it removes $\Sigma_1 - \Sigma_2$ from the denominator in (25) and gives for the nuclear distortion factor the Fourier transform (40) which is a product of the manifestly positive defined nuclear WW gluon distributions. Finally, the jet-jet inclusive cross section takes the form

$$\begin{aligned} \frac{d\sigma_{in}}{d^2 \mathbf{b} dz d\mathbf{p}_{-} d\boldsymbol{\Delta}} &= \frac{1}{2(2\pi)^2} \alpha_S \sigma_0 T(\mathbf{b}) \int_0^1 d\beta \int d^2 \boldsymbol{\kappa}_1 d^2 \boldsymbol{\kappa}_2 d^2 \boldsymbol{\kappa}_3 d^2 \boldsymbol{\kappa} f(\boldsymbol{\kappa}) \\ &\times \Phi(\beta \nu_A(\mathbf{b}), \boldsymbol{\Delta} - \boldsymbol{\kappa}_3 - \boldsymbol{\kappa}) \Phi(\beta \nu_A(\mathbf{b}), \boldsymbol{\kappa}_3) \end{aligned}$$

$$\begin{aligned}
& \times \Phi((1-\beta)\nu_A(\mathbf{b}), \boldsymbol{\kappa}_1)\Phi((1-\beta)\nu_A(\mathbf{b}), \boldsymbol{\kappa}_2) \\
& \times \{\langle\gamma^*|z, \mathbf{p}_- + \boldsymbol{\kappa}_2 + \boldsymbol{\kappa}_3\rangle - \langle\gamma^*|z, \mathbf{p}_- + \boldsymbol{\kappa}_2 + \boldsymbol{\kappa}_3 + \boldsymbol{\kappa}\rangle\} \\
& \times \{\langle z, \mathbf{p}_- + \boldsymbol{\kappa}_1 + \boldsymbol{\kappa}_3|\gamma^*\rangle - \langle z, \mathbf{p}_- + \boldsymbol{\kappa}_1 + \boldsymbol{\kappa}_3 + \boldsymbol{\kappa}|\gamma^*\rangle\} \\
& = \frac{1}{2(2\pi)^2}\alpha_S\sigma_0T(\mathbf{b})\int_0^1 d\beta\int d^2\boldsymbol{\kappa}_3d^2\boldsymbol{\kappa}f(\boldsymbol{\kappa}) \\
& \times \Phi(\beta\nu_A(\mathbf{b}), \boldsymbol{\Delta} - \boldsymbol{\kappa}_3 - \boldsymbol{\kappa})\Phi(\beta\nu_A(\mathbf{b}), \boldsymbol{\kappa}_3) \\
& \times \left|\int d^2\boldsymbol{\kappa}_1\Phi((1-\beta)\nu_A(\mathbf{b}), \boldsymbol{\kappa}_1)\right. \\
& \left.\times \{\langle\gamma^*|z, \mathbf{p}_- + \boldsymbol{\kappa}_1 + \boldsymbol{\kappa}_3\rangle - \langle\gamma^*|z, \mathbf{p}_- + \boldsymbol{\kappa}_1 + \boldsymbol{\kappa}_3 + \boldsymbol{\kappa}\rangle\}\right|^2. \quad (41)
\end{aligned}$$

This is our central result for inclusive cross section of the photon breakup into dijets off nuclei. It demonstrates how the broadening of the transverse momentum distribution of dijets is uniquely calculable in terms of the collective WW glue of a nucleus and as such must be regarded as a nonlinear k_\perp -factorization for inclusive dijet cross section.

The last form of (41) shows clearly that the integrand is manifestly positive valued. Going back to (39) and (40) one can identify the convolution of the collective nuclear WW glue $\Phi((1-\beta)\nu_A(\mathbf{b}), \boldsymbol{\kappa}_1)$ with the photon wave functions in the last form of (41) as an effect of distortions of the photon wave function when $q\bar{q}$ pair was propagating in still the color-singlet state.

Finally, consider the limiting case of $|\mathbf{p}_-|, |\boldsymbol{\Delta}| \lesssim Q_A$. In our analysis [5] of the single particle spectrum we discovered that the transverse momentum distribution of sea quarks is dominated by the anticollinear, anti-DGLAP splitting of gluons into sea, when the transverse momentum of the parent gluons is larger than the momentum of the sea quarks. As we stated in the Introduction, that suggests strongly a complete azimuthal decorrelation of forward minijets with the transverse momenta below the saturation scale, $p_\pm \lesssim Q_A$. Our analysis of $f^{(j)}(\boldsymbol{\kappa})$ in Appendix C shows that for average DIS on realistic nuclei Q_A^2 does not exceed several $(GeV/c)^2$, hence this regime is a somewhat academic one, see however the subsequent section 6. Still, let us assume that Q_A is so large that jets with $p_\pm \lesssim Q_A$ are measurable.

Notice, that $|\boldsymbol{\kappa}_i| \sim Q_A$, so that one can neglect \mathbf{p}_- in the photon's wave functions and the decorrelation momentum $\boldsymbol{\Delta}$ in the argument of $\Phi(\beta\nu_A(\mathbf{b}), \boldsymbol{\Delta} - \boldsymbol{\kappa}_3 - \boldsymbol{\kappa})$. Then an approximation

$$\begin{aligned}
& \left|\int d^2\boldsymbol{\kappa}_1\Phi((1-\beta)\nu_A(\mathbf{b}), \boldsymbol{\kappa}_1)\{\langle\gamma^*|z, \mathbf{p}_- + \boldsymbol{\kappa}_1 + \boldsymbol{\kappa}_3\rangle - \langle\gamma^*|z, \mathbf{p}_- + \boldsymbol{\kappa}_1 + \boldsymbol{\kappa}_3 + \boldsymbol{\kappa}\rangle\}\right|^2 \\
& \approx \left|\langle\gamma^*|z, \boldsymbol{\kappa}_3\rangle - \langle\gamma^*|z, \boldsymbol{\kappa}_3 + \boldsymbol{\kappa}\rangle\right|^2 \quad (42)
\end{aligned}$$

will be justified in (41). The principal point is that the minijet-minijet inclusive cross section depends on neither the minijet nor decorrelation momentum, which proves a disappearance of the azimuthal decorrelation of minijets with the transverse momentum below the saturation scale.

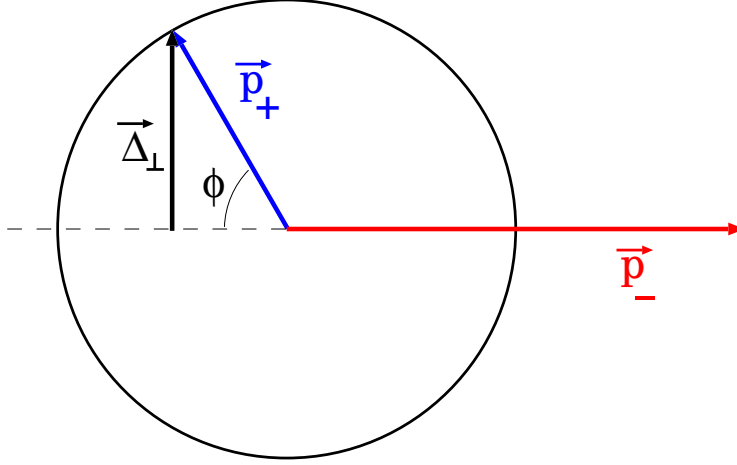


Figure 3: The definition of the considered dijet configurations and of the transverse component of the acoplanarity momentum Δ_{\perp} .

6 Azimuthal decorrelation of dijets in DIS off nuclei: numerical estimates

The azimuthal decorrelation of two jets is quantified by the mean transverse acoplanarity momentum squared $\langle \Delta_{\perp}^2(\mathbf{b}) \rangle$, where Δ_{\perp} is transverse to an axis of the jet with higher momentum, see fig. 3. Here we present numerical estimates for hard dijets, $|\mathbf{p}_+| \gg Q_A$. The convolution property of the hard dijet cross section (35) suggests

$$\begin{aligned} \langle \Delta_{\perp}^2(\mathbf{b}) \rangle_A &= \left\{ \int_{\mathcal{C}} d^2\mathbf{p}_- \Delta_{\perp}^2 \frac{d\sigma_N}{dz d^2\mathbf{p}_+ d^2\mathbf{p}_-} \right\} / \left\{ \int_{\mathcal{C}} d^2\mathbf{p}_- \frac{d\sigma_N}{dz d^2\mathbf{p}_+ d^2\mathbf{p}_-} \right\} \\ &\approx \langle \kappa_{\perp}^2(\mathbf{b}) \rangle_A + \langle \Delta_{\perp}^2 \rangle_N, \end{aligned} \quad (43)$$

where $\langle \Delta_{\perp}^2 \rangle_N$ refers to DIS on a free nucleon, and $\langle \kappa_{\perp}^2(\mathbf{b}) \rangle_A$ is the nuclear broadening term

$$\langle \kappa_{\perp}^2(\mathbf{b}) \rangle_A = \left\{ \int_{\mathcal{C}} d^2\kappa \kappa_{\perp}^2 \Phi(2\beta\lambda_c\nu_A(\mathbf{b}), \kappa) \right\} / \left\{ \int_{\mathcal{C}} d^2\kappa \Phi(2\beta\lambda_c\nu_A(\mathbf{b}), \kappa) \right\}. \quad (44)$$

The sign \approx in (43) reflects the kinematical limitations \mathcal{C} on \mathbf{p}_- and κ in the practical evaluation of the acoplanarity distribution. In a typical final state shown in fig. 3 it is the harder jet with larger transverse momentum which defines the jet axis and the acoplanarity momentum Δ will be defined in terms of components of the momentum of softer jet with respect to that axis, for instance, see [20]. For the sake of definiteness, we present numerical estimates for the Gedanken experiment in which we classify the event as a dijet if the quark and antiquark are produced in different hemispheres, i.e., if the azimuthal angle ϕ between two jets exceeds $\pi/2$, the quark jet has fixed $|\mathbf{p}_+|$ and the antiquark jet has higher transverse momentum $|\mathbf{p}_+| \lesssim |\mathbf{p}_-| \lesssim 10|\mathbf{p}_+|$ (in the discussion

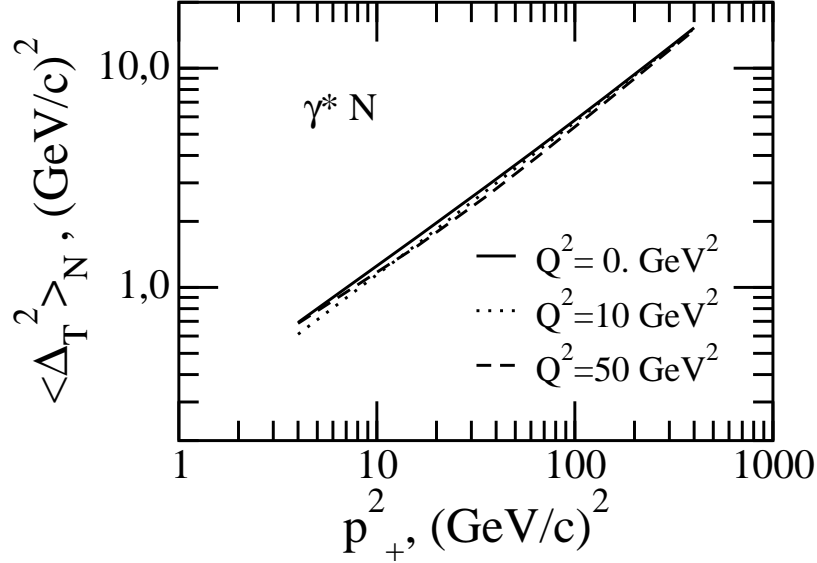


Figure 4: The mean acoplanarity momentum squared $\langle \Delta_{\perp}^2 \rangle_N$ for DIS on a free nucleon target with production of trigger jets with the transverse momentum higher than \mathbf{p}_+ for several values of Q^2 . The numerical results are for $x = 0.01$ and the input unintegrated gluon structure of the proton is taken from ref. [19].

of the experimental data one often refers to the higher momentum jet as the trigger jet and the softer jet as the away jet [20]).

The free-nucleon quantity $\langle \Delta_{\perp}^2 \rangle_N$ is evaluated from eq. (43) with the free nucleon cross section (7). For the evaluation purposes one can start with the small- Δ expansion for excitation of hard, $\mathbf{p}_+^2 \gg \varepsilon^2 = z(1-z)Q^2$, light flavor dijets from transverse photons

$$\begin{aligned} \frac{d\sigma_N}{dzd^2\mathbf{p}_+d^2\Delta} &\approx \frac{1}{\pi} e_f^2 \alpha_{em} \alpha_S(\mathbf{p}_+^2) [z^2 + (1-z)^2] \\ &\times \frac{1}{\Delta^4} \cdot \frac{\partial G(x, \Delta^2)}{\partial \log \Delta^2} \cdot \frac{\Delta^2}{(\varepsilon^2 + \mathbf{p}_+^2)(\varepsilon^2 + \mathbf{p}_+^2 + \Delta^2)}. \end{aligned} \quad (45)$$

The form of the last factor in (45) only mimics its leveling off at $\Delta^2 \gtrsim \mathbf{p}_+^2$, see eq. (7). Then in the denominator of (43) one finds the typical logarithmic integral

$$\frac{1}{\pi} \int_0^\pi d\phi \int^{\mathbf{p}_+^2} \frac{d\Delta^2}{\Delta^2} \cdot \frac{\partial G(x, \Delta^2)}{\partial \log \Delta^2} = G(x, \mathbf{p}_+^2) \quad (46)$$

compared to the numerator of the form

$$\frac{1}{\pi} \int_0^\pi d\phi \sin^2 \phi \int^{\mathbf{p}_+^2} d\Delta^2 \cdot \frac{\partial G(x, \Delta^2)}{\partial \log \Delta^2} \sim \frac{1}{2} \mathbf{p}_+^2 \mathcal{F}(x, \mathbf{p}_+^2). \quad (47)$$

More accurate numerical estimates for the selection criteria of our Gedanken experiment suggest the numerical factor ≈ 0.7 in (47) and

$$\begin{aligned} \langle \Delta_\perp^2 \rangle_N &= \left\{ \int_{p_+} d^2 \mathbf{p}_- \Delta_\perp^2 \frac{d\sigma_N}{dz d^2 \mathbf{p}_+ d^2 \mathbf{p}_-} \right\} / \left\{ \int_{p_+} d^2 \mathbf{p}_- \frac{d\sigma_N}{dz d^2 \mathbf{p}_+ d^2 \mathbf{p}_-} \right\} \\ &\approx 0.7 \cdot \frac{\mathcal{F}(x, \mathbf{p}_+^2)}{G(x, \mathbf{p}_+^2)} \mathbf{p}_+^2, \end{aligned} \quad (48)$$

correctly describes the numerical results shown in fig. 4. As far as the dijets are hard, $\mathbf{p}_+^2 \gtrsim z(1-z)Q^2 \sim \frac{1}{4}Q^2$, the acoplanarity momentum distribution would not depend on Q^2 , which holds still better if one considers $\sigma_T + \sigma_L$. This point is illustrated in fig. 4, where we show $\langle \Delta_\perp^2 \rangle_N$ at $z = 1/2$ for several values of Q^2 . Because of this weak dependence on Q^2 herebelow we make no distinction between DIS and real photoproduction, $Q^2 = 0$.

In the practical evaluations of the nuclear contribution $\langle \kappa_\perp^2(\mathbf{b}) \rangle_A$ one can use an explicit expansion

$$\int_0^1 d\beta \Phi(2\beta \lambda_c \nu_A(\mathbf{b}), \boldsymbol{\kappa}) = \sum_{j=0}^{\infty} w_A(\mathbf{b}, j) f^{(j)}(\boldsymbol{\kappa}) = \sum_{j=0}^{\infty} \frac{1}{j!} \frac{\gamma(j+1, 2\lambda_c \nu_A(\mathbf{b}))}{2\lambda_c \nu_A(\mathbf{b})} f^{(j)}(\boldsymbol{\kappa}), \quad (49)$$

where $\gamma(j, x) = \int_0^x dy y^{j-1} \exp(-y)$ is an incomplete gamma-function. The properties of the collective glue for j overlapping nucleons, $f^{(j)}(\boldsymbol{\kappa})$, are presented in Appendix C. For a heavy nucleus (49) can be approximated by its integrand at $\beta \approx 1/2$, ie., by $\Phi(\lambda_c \nu_A(\mathbf{b}), \boldsymbol{\kappa})$. A bit more accurate evaluation of the numerically important no-broadening contribution from $j = 0$ gives

$$\int_0^1 d\beta \Phi(2\beta \lambda_c \nu_A(\mathbf{b}), \boldsymbol{\kappa}) \approx w_A(\mathbf{b}, 0) \delta(\boldsymbol{\kappa}) + (1 - w_A(\mathbf{b}, 0)) \frac{1}{\pi} \frac{\lambda_c Q_A^2(\mathbf{b})}{(\boldsymbol{\kappa}^2 + \lambda_c Q_A^2(\mathbf{b}))^2} \quad (50)$$

where Q_A^2 is given by eq. (108) and

$$w_A(\mathbf{b}, 0) = \frac{1 - \exp[-\nu_A(\mathbf{b})]}{\nu_A(\mathbf{b})} \quad (51)$$

is a probability of the no-broadening contribution, which for realistic nuclei is still substantial. In our Gedanken experiment $\langle \kappa_\perp^2(\mathbf{b}) \rangle_A$ must be evaluated over the constrained

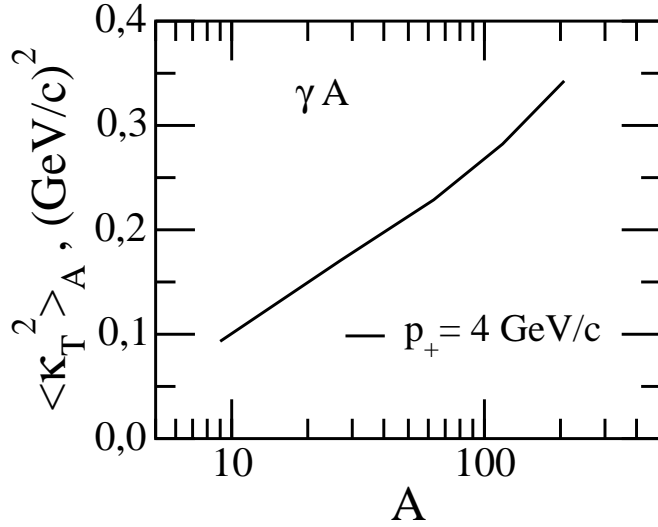


Figure 5: *The atomic mass number dependence of nuclear broadening contribution, $\langle \kappa_{\perp}^2(\mathbf{b}) \rangle_A$, to the mean acoplanarity momentum squared for real photoproduction off nuclei at $x = 0.01$. The input unintegrated gluon SF of the proton is taken from ref. [19].*

phase space \mathcal{C} , $\kappa_{\perp} \leq |\mathbf{p}_+|$ and $\kappa_L > 0$, and the analytic parameterization (50) gives

$$\begin{aligned}
 \langle \kappa_{\perp}^2(\mathbf{b}) \rangle_A &\approx \lambda_c Q_A^2(\mathbf{b}) \cdot \left[\log \tan \left(\frac{\pi}{4} + \frac{1}{2} \arctan \frac{p_+}{\sqrt{\lambda_c Q_A^2(\mathbf{b})}} \right) - \frac{p_+}{\sqrt{\lambda_c Q_A^2(\mathbf{b}) + p_+^2}} \right] \\
 &\times \frac{(1 - w_A(\mathbf{b}, 0)) \sqrt{\lambda_c Q_A^2(\mathbf{b}) + p_+^2}}{w_A(\mathbf{b}, 0) \sqrt{\lambda_c Q_A^2(\mathbf{b}) + p_+^2} + (1 - w_A(\mathbf{b}, 0)) p_+}. \quad (52)
 \end{aligned}$$

We recall that (43) and (52) must only be used for $|\mathbf{p}_+| \gg Q_A(\mathbf{b})$.

For average DIS on heavy nuclei the reference value is $\langle Q_{Au}^2(\mathbf{b}) \rangle = 0.9 (\text{GeV}/c)^2$, see Appendix C. The atomic mass number dependence of nuclear broadening $\langle \kappa_{\perp}^2 \rangle_A$ for jets

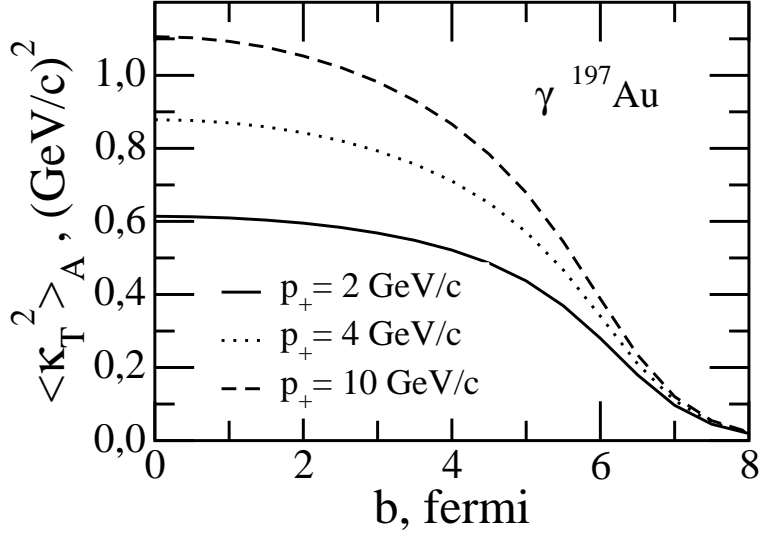


Figure 6: *The impact parameter dependence of the nuclear broadening contribution, $\langle \kappa_{\perp}^2(\mathbf{b}) \rangle_A$, to the mean acoplanarity momentum squared from peripheral DIS at large impact parameter to central DIS at $\mathbf{b} = 0$ for several values of the away jet momentum p_+ . The numerical results are for $x = 0.01$ and the input unintegrated gluon SF of the proton is taken from ref. [19].*

with $p_+ = 4$ GeV/c in average DIS off nucleus is shown in fig. 5. The principal reason why $\langle \kappa_{\perp}^2 \rangle_A$ is numerically small compared to $\langle Q_{Au}^2(\mathbf{b}) \rangle$ is that even for such a heavy nucleus as ^{197}Au the no-broadening probability in average DIS is large, $\langle w_{Au}(\mathbf{b}, 0) \rangle \approx 0.5$. A comparison of the free nucleon broadening $\langle \Delta_{\perp}^2 \rangle_N$ from fig. 4 with the nuclear contribution $\langle \kappa_{\perp}^2(\mathbf{b}) \rangle_A$ from fig. 5 shows suggest that the nuclear mass number dependence of azimuthal decorrelation of dijets in average DIS off nuclei will be relatively weak.

However, nuclear broadening will be substantially stronger for a subsample of central DIS events at $\mathbf{b} \sim 0$. In fig. 6 we show for the gold, ^{197}Au , target a dependence of the β averaged nuclear broadening $\langle \kappa_{\perp}^2(\mathbf{b}) \rangle_A$ on the impact parameter at several values of p_+ .

There are two related sources of the p_+ dependence of $\langle \kappa_{\perp}^2(\mathbf{b}) \rangle_A$. First, since for hard dijets $r, r' \sim 1/p_+$, the strong coupling enters eq. (33) and eq. (108) as $\alpha_S(\mathbf{p}_+^2)$. Then for hard jets $\nu_A(\mathbf{b}) \propto \alpha_S(\mathbf{p}_+^2)$ and $w_A(\mathbf{b} = 0, 0)$ rises substantially with p_+ in the region of p_+ of the practical interest, $1 \lesssim p_+ \lesssim (5-10)$ GeV/c, where the strong coupling varies rapidly. For a nucleus with mass number $A = 200$ it rises from $w_A(\mathbf{b} = 0, 0) \approx 0.12$ at $p_+ = 2$ GeV/c to ≈ 0.20 at 4 GeV/c to ≈ 0.25 at $p_+ = 10$ GeV/c (for the nuclear density parameterization see [39]). Second, for the same reason that $\nu_A(\mathbf{b}) \propto \alpha_S(\mathbf{p}_+^2)$ the contribution from large j in (49), and $Q_A^2(\mathbf{b})$ thereof, diminish gradually with rising p_+ , proportionally to $\alpha_S(\mathbf{p}_+^2)/\alpha_S(Q_A^2)$. In the region of $p_+ \lesssim 10$ GeV/c of the practical interest one finds $\langle \kappa_{\perp}^2(\mathbf{b}) \rangle_A \sim Q_A^2(\mathbf{b})$.

Now compare the numerical results in fig. 5 and fig. 6 for $p_+ = 4$ GeV/c and ^{197}Au target. According to eq. (109) of Appendix C,

$$Q_A^2(0) = \left(\frac{4}{3} - 2\right) \langle Q_A^2(\mathbf{b}) \rangle. \quad (53)$$

The no-broadening probability $w_{Au}(\mathbf{b}, 0)$ for central DIS is substantially smaller, $w_A(\mathbf{b} = 0, 0) \approx 0.20$, than for average DIS, $\langle w_{Au}(\mathbf{b}, 0) \rangle \approx 0.5$. In conjunction with (53) that entails an enhancement of $\langle \kappa_{\perp}^2(\mathbf{b}) \rangle_A$ by the factor of $\sim (2.5 - 3)$ from average to central DIS. The same point is illustrated by the expectation value of j in (49) for the Au target, which for jets with $p_+ = 4$ GeV/c drops the the factor ~ 3 from $\langle j(\mathbf{b} = 0) \rangle = 2.86$ to $\langle j \rangle_A = 0.87$ from central to average DIS.

One can enhance Q_A^2 and nuclear contribution $\langle \kappa_{\perp}^2(\mathbf{b}) \rangle_A$ still further selecting DIS events when the photon breaks up into the $q\bar{q}$ pair on the front face of a nucleus, which in the language of (36) corresponds to the contribution from $\beta \rightarrow 1$, see the discussion of (49). Experimentally, precisely such events are isolated by selecting very large multiplicity or very high transverse energy of produced secondary particles ([20] and references therein). Then, eq. (36), shows, (see also a discussion of $\beta \approx 1/2$ approximation in (49)) that for very high multiplicity central DIS off Au nucleus $Q_A^2 \sim 2.5$ GeV² is quite feasible. Eq. (52) shows that for such a large $Q_A^2 \sim 2.5$ GeV² and $p_+ = (5-10)$ GeV of the practical interest $\langle \kappa_{\perp}^2(\mathbf{b} = 0) \rangle$ grows slower than $\propto Q_A^2$, so that for high-multiplicity central DIS off Au nucleus the value of $\langle \kappa_{\perp}^2(\mathbf{b} = 0) \rangle$ will be enhanced by the factor $\sim (4-5)$ from $\langle \kappa_{\perp}^2 \rangle_{Au}$ for average DIS.

We have an overall good understanding of gross features of nuclear azimuthal decorrelations in DIS off nuclei. Now we comment on the recent finding by the STAR collaboration of a disappearance of back-to-back high p_{\perp} hadron correlation when going from peripheral to central gold-gold collisions at RHIC [20]. Our experience with application of color dipole formalism to hard hadron-nucleus interactions [17] suggests that our analysis of acoplanarity of forward hard jets can be readily generalized to mid-rapidity jets. One only has to choose an appropriate system of dipoles, for instance, the open heavy flavor production can be treated in terms of the intranuclear propagation of the gluon-quark-antiquark system in the overall color-singlet state. At RHIC energies jets with moderately large p_{\perp} are for the most part due to gluon-gluon collisions. In our language that can be treated as a breakup of gluons into dijets and azimuthal decorrelation of hard jets must be discussed in terms of intranuclear propagation of color-octet gluon-gluon

dipoles. For such gluon-gluon dipoles the relevant saturation scale Q_{sA}^2 is larger [24] than that for the quark-antiquark dipoles by the factor $2\lambda_c = C_A/C_F = 9/4$. Arguably, in central nucleus-nucleus collisions distortions in the target and projectile nuclei add up and the effective thickness of nuclear matter is about twice that in DIS. Then, the results shown in fig. 5 suggest that for central gold-gold collisions the nuclear broadening of gluon-gluon dijets could be quite substantial, $\langle \kappa_{\perp}^2(\mathbf{b} = 0) \rangle_{AuAu} \sim (3-4) (GeV/c)^2$ for average central $AuAu$ collisions and even twice larger if collisions take place at front surface of colliding nuclei.

The principal effect of nuclear broadening is a reduction of the probability of observing the back-to-back jets

$$\propto \frac{\langle \Delta_{\perp}^2 \rangle_N}{\langle \kappa_{\perp}^2(\mathbf{b}) \rangle_A + \langle \Delta_{\perp}^2 \rangle_N} \quad (54)$$

and one needs to compare $\langle \Delta_{\perp}^2 \rangle_N$ to $\langle \kappa_{\perp}^2(\mathbf{b}) \rangle_A$. Our eq. (48) for the free nucleon case holds as well for the gluon-gluon collisions. Then the results shown in fig. 3 entail that $\langle \Delta_{\perp}^2 \rangle_N \approx \langle \kappa_{\perp}^2(0) \rangle_{AuAu} \sim (3-4) (GeV/c)^2$ at the jet momentum $p_+ = p_J = (6-8) GeV/c$ and our nuclear broadening would become substantial for all jets with p_+ below the decorrelation threshold momentum p_J . In practice, the STAR collaboration studied the azimuthal correlation of two high- p_{\perp} hadrons and for the quantitative correspondence between the STAR observable and azimuthal decorrelation in the parent dijet one needs to model fragmentation of jets into hadrons (for the modern fragmentation schemes see [35]), here we notice that the cutoff p_+ in our Gedanken experiment is related to the momentum cutoff $p_{T,min}$ of associated tracks from the away jet, whereas our jet of momentum \mathbf{p}_- can be regarded as a counterpart of the trigger jet of STAR. The STAR cutoff $p_T = 2 GeV/c$ corresponds to the parents jets with the transverse momentum $p_+ \sim (2-3)p_T = (4-6) GeV$ which is comparable to, or even smaller than, the decorrelation threshold momentum $p_J = (6-8) GeV/c$. Then eq. (54) suggests that in the kinematics of STAR the probability to observe the back-to-back away and trigger jets decreases approximately twofold, and perhaps even stronger, from peripheral to central $AuAu$ collisions, so that our azimuthal decorrelation may contribute substantially to the STAR effect.

In practical consideration of azimuthal decorrelations in central heavy ion collisions the above distortions of the produced jet-jet inclusive spectrum due to interactions with the nucleons of the target and projectile ions must be complemented by rescatterings of parent high- p_{\perp} partons on the abundantly produced secondary hadrons. Our nuclear decorrelation effect will be the dominant one and reinteractions with secondary particles will be marginal in pA collisions, where for central collisions we expect $\langle \kappa_{\perp}^2(0) \rangle_{pAu} \sim 1.5 (GeV/c)^2$ and for central collisions in the regime of $\beta \rightarrow 1$, i.e., with limiting high multiplicity even $\langle \kappa_{\perp}^2(0) \rangle_{pAu} \sim 3 (GeV/c)^2$ is feasible.

7 Nuclear k_{\perp} -factorization for $1/N_c^2$ corrections to the photon breakup

Having established nuclear k_{\perp} -factorization properties of dijet cross section to leading order of the large- N_c approximation, we turn to the $1/N_c^2$ corrections and demonstrate that with one simple exception the $1/N_c^2$ expansion can be regarded as the higher-twist expansion. The two sources of the $1/N_c^2$ corrections to the nuclear distortion factor are higher order terms in the off-diagonal σ_{18} and the $\propto 1/(N_c^2 - 1)$ terms in σ_{88} , eq. (21). To this end we notice that σ_{88} can be decomposed as

$$\begin{aligned}\sigma_{88} &= \sigma(\mathbf{s}) + \sigma(\mathbf{s} - \mathbf{r} + \mathbf{r}') + \frac{2\Sigma_{18}(\mathbf{s}, \mathbf{r}, \mathbf{r}')}{N_c^2 - 1} \\ &+ \frac{\sigma(\mathbf{s}) + \sigma(\mathbf{s} - \mathbf{r} + \mathbf{r}') - \sigma(\mathbf{r}) - \sigma(\mathbf{r}')}{N_c^2 - 1} \\ &= \frac{N_c^2}{N_c^2 - 1} [\sigma(\mathbf{s}) + \sigma(\mathbf{s} - \mathbf{r} + \mathbf{r}')] + \frac{2\Sigma_{18}(\mathbf{s}, \mathbf{r}, \mathbf{r}')}{N_c^2 - 1} - \frac{\Delta\Sigma_{88}(\mathbf{r}, \mathbf{r}')}{N_c^2 - 1},\end{aligned}\quad (55)$$

where

$$\Delta\Sigma_{88}(\mathbf{r}, \mathbf{r}') = \sigma(\mathbf{r}) + \sigma(\mathbf{r}') \quad (56)$$

and we exactly reabsorbed one part of the $1/N_c^2$ correction into the leading large- N_c term of σ_{88} scaling it up by the color factor λ_c .

After some algebra one finds

$$\begin{aligned}\langle 11|S_{4A}(\mathbf{b}'_+, \mathbf{b}'_-, \mathbf{b}_+, \mathbf{b}_-)|11\rangle &= \exp\left\{-\frac{1}{2}[\sigma(\mathbf{r}) + \sigma(\mathbf{r}')]T(\mathbf{b})\right\} \\ &+ \frac{\Sigma_{18}^2(\mathbf{s}, \mathbf{r}, \mathbf{r}')T^2(\mathbf{b})}{4(N_c^2 - 1)} \int_0^1 d\beta \int_0^\beta d\beta_1 \\ &\times \exp\left\{-\frac{1}{2}(1 - \beta + \beta_1)[\sigma(\mathbf{r}) + \sigma(\mathbf{r}')]T(\mathbf{b})\right\} \\ &\times \exp\left\{-\frac{1}{2}(\beta - \beta_1)[\sigma(\mathbf{s}) + \sigma(\mathbf{s} - \mathbf{r} + \mathbf{r}')]T(\mathbf{b})\right\}.\end{aligned}\quad (57)$$

Notice, that the first term in (57) is cancelled by the subtraction of the coherent diffractive term (22) in (8), (25), so that only the subleading, $\propto 1/(N_c^2 - 1)$ term in (57) contributes to the dijet cross section. The evaluation of corrections to the leading term of the Sylvester expansion is a bit more complicated:

$$\begin{aligned}\sqrt{N_c^2 - 1}\langle 88|S_{4A}(\mathbf{b}'_+, \mathbf{b}'_-, \mathbf{b}_+, \mathbf{b}_-)|11\rangle &= \frac{1}{2}\Sigma_{18}(\mathbf{s}, \mathbf{r}, \mathbf{r}')T(\mathbf{b}) \\ &\times \left[\int_0^1 d\beta \exp\left\{-\frac{1}{2}\beta[\sigma(\mathbf{r}) + \sigma(\mathbf{r}')]T(\mathbf{b})\right\} \exp\left\{-\frac{1}{2}(1 - \beta)\sigma_{88}T(\mathbf{b})\right\}\right. \\ &+ \left.\frac{\Sigma_{18}^2(\mathbf{s}, \mathbf{r}, \mathbf{r}')T^2(\mathbf{b})}{4(N_c^2 - 1)} \int_0^1 d\beta \int_0^\beta d\beta_1 \int_0^{\beta_1} d\beta_2\right.\end{aligned}$$

$$\begin{aligned}
& \times \exp \left\{ -\frac{1}{2}(\beta - \beta_1 + \beta_2)[\sigma(\mathbf{r}) + \sigma(\mathbf{r}')T(\mathbf{b})] \right\} \\
& \times \exp \left\{ -\frac{1}{2}(1 - \beta + \beta_1 - \beta_2)[\sigma(\mathbf{s}) + \sigma(\mathbf{s} - \mathbf{r} + \mathbf{r}')T(\mathbf{b})] \right\} \Bigg]. \quad (58)
\end{aligned}$$

The first term of (58) contains the attenuation factor where σ_{88} is still an exact diagonal matrix element, and one must isolate the leading term and $1/(N_c^2 - 1)$ correction:

$$\begin{aligned}
& \exp \left\{ -\frac{1}{2}(1 - \beta)\sigma_{88}T(\mathbf{b}) \right\} = \exp \left\{ -\frac{1}{2}(1 - \beta)\lambda_c[\sigma(\mathbf{s}) + \sigma(\mathbf{s} - \mathbf{r} + \mathbf{r}')T(\mathbf{b})] \right\} \\
& \times \left\{ 1 - \frac{(1 - \beta)\Sigma_{18}(\mathbf{s}, \mathbf{r}, \mathbf{r}')T(\mathbf{b})}{N_c^2 - 1} + \frac{(1 - \beta)\Delta\Sigma_{88}(\mathbf{r}, \mathbf{r}')T(\mathbf{b})}{2(N_c^2 - 1)} \right\}. \quad (59)
\end{aligned}$$

The fundamental reason why the different components of the second term $\propto 1/(N_c^2 - 1)$ in eq. (21) were treated differently is that the NSS representation with positive valued Fourier transform only holds for attenuating exponentials of the dipole cross section. One can readily write down the related expansion for rising exponential $\exp[\frac{1}{2}\sigma(\mathbf{r})T(\mathbf{b})]$, but its Fourier transform shall be a sign-oscillating expansion:

$$\exp \left[\frac{1}{2}\sigma(\mathbf{s})T(\mathbf{b}) \right] = \exp [2\nu_A(\mathbf{b})] \sum_{j=0}^{\infty} (-1)^j w_j(\nu_A(\mathbf{b})) \int d^2\boldsymbol{\kappa} f^{(j)}(\boldsymbol{\kappa}) \exp(i\boldsymbol{\kappa}\mathbf{s}). \quad (60)$$

For this reason combining together in the first term of (57) the two exponentials with similar exponents $\propto [\sigma(\mathbf{r}) + \sigma(\mathbf{r}')]T(\mathbf{b})$ is not warranted, because in the course of the β integration the sign of the exponent will change from attenuation to growth,

$$\beta[\sigma(\mathbf{r}) + \sigma(\mathbf{r}')] - \frac{1}{N_c^2 - 1}(1 - \beta)\Delta\Sigma_{88}(\mathbf{r}, \mathbf{r}') = \frac{N_c^2\beta - 1}{N_c^2 - 1}[\sigma(\mathbf{r}) + \sigma(\mathbf{r}')], \quad (61)$$

and it is advisable to stick to the perturbative expansion (59).

The final result for the nuclear absorption factor to an accuracy $1/(N_c^2 - 1)$ reads

$$\begin{aligned}
D_A(\mathbf{s}, \mathbf{r}, \mathbf{r}', \mathbf{b}) &= \frac{\Sigma_{18}(\mathbf{s}, \mathbf{r}, \mathbf{r}')T(\mathbf{b})}{2(N_c^2 - 1)} \int_0^1 d\beta \int_0^\beta d\beta_1 \\
&\times \exp \left\{ -\frac{1}{2}(1 - \beta + \beta_1)[\sigma(\mathbf{r}) + \sigma(\mathbf{r}')T(\mathbf{b})] \right\} \\
&\times \exp \left\{ -\frac{1}{2}(\beta - \beta_1)[\sigma(\mathbf{s}) + \sigma(\mathbf{s} - \mathbf{r} + \mathbf{r}')T(\mathbf{b})] \right\} \quad (62) \\
&+ \frac{\Sigma_{18}^2(\mathbf{s}, \mathbf{r}, \mathbf{r}')T^2(\mathbf{b})}{4(N_c^2 - 1)} \int_0^1 d\beta \int_0^\beta d\beta_1 \int_0^{\beta_1} d\beta_2 \\
&\times \exp \left\{ -\frac{1}{2}(\beta - \beta_1 + \beta_2)[\sigma(\mathbf{r}) + \sigma(\mathbf{r}')T(\mathbf{b})] \right\} \\
&\times \exp \left\{ -\frac{1}{2}(1 - \beta + \beta_1 - \beta_2)[\sigma(\mathbf{s}) + \sigma(\mathbf{s} - \mathbf{r} + \mathbf{r}')T(\mathbf{b})] \right\} \quad (63) \\
&- \frac{\Sigma_{18}(\mathbf{s}, \mathbf{r}, \mathbf{r}')T(\mathbf{b})}{N_c^2 - 1} \int_0^1 d\beta(1 - \beta)
\end{aligned}$$

$$\begin{aligned}
& \times \exp \left\{ -\frac{1}{2}\beta[\sigma(\mathbf{r}) + \sigma(\mathbf{r}')T(\mathbf{b})] \right\} \\
& \times \exp \left\{ -\frac{1}{2}(1-\beta)\lambda_c[\sigma(\mathbf{s}) + \sigma(\mathbf{s} - \mathbf{r} + \mathbf{r}')T(\mathbf{b})] \right\} \tag{64}
\end{aligned}$$

$$\begin{aligned}
& + \frac{\Delta\Sigma_{88}(\mathbf{r}, \mathbf{r}')T(\mathbf{b})}{2(N_c^2 - 1)} \int_0^1 d\beta(1-\beta) \\
& \times \exp \left\{ -\frac{1}{2}\beta[\sigma(\mathbf{r}) + \sigma(\mathbf{r}')T(\mathbf{b})] \right\} \\
& \times \exp \left\{ -\frac{1}{2}(1-\beta)\lambda_c[\sigma(\mathbf{s}) + \sigma(\mathbf{s} - \mathbf{r} + \mathbf{r}')T(\mathbf{b})] \right\} \tag{65}
\end{aligned}$$

$$\begin{aligned}
& + \int_0^1 d\beta \exp \left\{ -\frac{1}{2}(1-\beta)[\sigma(\mathbf{r}) + \sigma(\mathbf{r}')T(\mathbf{b})] \right\} \\
& \times \exp \left\{ -\frac{1}{2}\beta[\sigma(\mathbf{s}) + \sigma(\mathbf{s} + \mathbf{r}' - \mathbf{r})T(\mathbf{b})] \right\}. \tag{66}
\end{aligned}$$

Here the last term (66) is the leading large- N_c result, the first (62) and second (63) terms describe contributions to the dijet cross section of second and third order in the off-diagonal σ_{18} , the third (64) and fourth (65) term come from the expansion (59).

As in illustration of salient features of $1/(N_c^2 - 1)$ corrections we expose in details the contribution from the first term (62). Following the considerations in sections 4 & 5, one readily obtains

$$\begin{aligned}
& \frac{d\Delta\sigma_{in}^{(1)}}{d^2\mathbf{b}dzd\mathbf{p}_-d\mathbf{\Delta}} = \frac{\alpha_S^2\sigma_0^2T^2(\mathbf{b})}{4(2\pi)^2(N_c^2 - 1)} \int_0^1 d\beta \int_0^\beta d\beta_1 \\
& \times \int d^2\mathbf{q}_1d^2\mathbf{q}_2d^2\boldsymbol{\kappa}_3f(\mathbf{q}_1)f(\mathbf{q}_2) \\
& \times \Phi((\beta - \beta_1)\nu_A(\mathbf{b}), \mathbf{\Delta} - \boldsymbol{\kappa}_3 - \mathbf{q}_1 - \mathbf{q}_2)\Phi((\beta - \beta_1)\nu_A(\mathbf{b}), \boldsymbol{\kappa}_3) \\
& \times \left| \int d^2\boldsymbol{\kappa}_1\Phi((1 - \beta + \beta_1)\nu_A(\mathbf{b}), \boldsymbol{\kappa}_1) \right. \\
& \times \left. \left\{ \langle \gamma^*|z, \mathbf{p}_- + \boldsymbol{\kappa}_1 + \boldsymbol{\kappa}_3 \rangle - \langle \gamma^*|z, \mathbf{p}_- + \boldsymbol{\kappa}_1 + \boldsymbol{\kappa}_3 + \mathbf{q}_1 \rangle \right. \right. \\
& \left. \left. - \langle \gamma^*|z, \mathbf{p}_- + \boldsymbol{\kappa}_1 + \boldsymbol{\kappa}_3 + \mathbf{q}_2 \rangle + \langle \gamma^*|z, \mathbf{p}_- + \boldsymbol{\kappa}_1 + \boldsymbol{\kappa}_3 + \mathbf{q}_1 + \mathbf{q}_2 \rangle \right\} \right|^2. \tag{67}
\end{aligned}$$

Of particular interest is the large- $|\mathbf{p}_-|$ behavior of (67). We notice that for $\mathbf{p}_-^2 \gg Q_A^2(\mathbf{b})$ one can neglect $\boldsymbol{\kappa}_{1,3}$ in the argument of the photon wave function, so that

$$\begin{aligned}
& \int d^2\boldsymbol{\kappa}_1\Phi((1 - \beta + \beta_1)\nu_A(\mathbf{b}), \boldsymbol{\kappa}_1) \\
& \times \left\{ \langle \gamma^*|z, \mathbf{p}_- + \boldsymbol{\kappa}_1 + \boldsymbol{\kappa}_3 \rangle - \langle \gamma^*|z, \mathbf{p}_- + \boldsymbol{\kappa}_1 + \boldsymbol{\kappa}_3 + \mathbf{q}_1 \rangle \right. \\
& \left. - \langle \gamma^*|z, \mathbf{p}_- + \boldsymbol{\kappa}_1 + \boldsymbol{\kappa}_3 + \mathbf{q}_2 \rangle + \langle \gamma^*|z, \mathbf{p}_- + \boldsymbol{\kappa}_1 + \boldsymbol{\kappa}_3 + \mathbf{q}_1 + \mathbf{q}_2 \rangle \right\} \\
& \approx \left\{ \langle \gamma^*|z, \mathbf{p}_- \rangle - \langle \gamma^*|z, \mathbf{p}_- + \mathbf{q}_1 \rangle - \langle \gamma^*|z, \mathbf{p}_- + \mathbf{q}_2 \rangle + \langle \gamma^*|z, \mathbf{p}_- + \mathbf{q}_1 + \mathbf{q}_2 \rangle \right\}, \tag{68}
\end{aligned}$$

where we used the normalization property $\int d^2\boldsymbol{\kappa}_1\Phi((1 - \beta + \beta_1)\nu_A(\mathbf{b}), \boldsymbol{\kappa}_1) = 1$. Next one

can readily verify that

$$\begin{aligned} & \int d^2\boldsymbol{\kappa}_3 \Phi((\beta - \beta_1)\nu_A(\mathbf{b}), \boldsymbol{\Delta} - \boldsymbol{\kappa}_3 - \mathbf{q}_1 - \mathbf{q}_2) \Phi((\beta - \beta_1)\nu_A(\mathbf{b}), \boldsymbol{\kappa}_3) \\ &= \Phi((\beta - \beta_1)\nu_A(\mathbf{b}), \boldsymbol{\Delta} - \mathbf{q}_1 - \mathbf{q}_2) \end{aligned} \quad (69)$$

Incidentally, by a similar analysis of the onset of high- \mathbf{p}_+ limit one would obtain the linear nuclear k_\perp -factorization (36) for hard dijets from the nonlinear nuclear k_\perp -factorization (41).

The combination of the photon wave functions in (68) corresponds to the second finite difference in $\mathbf{q}_1, \mathbf{q}_2$, so that for jets with $\mathbf{p}_-^2 \gg \varepsilon^2$ one has an estimate

$$\begin{aligned} & \left| \langle \gamma^* | z, \mathbf{p}_- \rangle - \langle \gamma^* | z, \mathbf{p}_- + \mathbf{q}_1 \rangle + \langle \gamma^* | z, \mathbf{p}_- + \mathbf{q}_2 \rangle - \langle \gamma^* | z, \mathbf{p}_- + \mathbf{q}_1 + \mathbf{q}_2 \rangle \right|^2 \\ & \approx \left| \langle \gamma^* | z, \mathbf{p}_- \rangle \right|^2 \cdot \frac{\mathbf{q}_1^2 \mathbf{q}_2^2}{(\mathbf{p}_-^2)^2} \end{aligned} \quad (70)$$

which shows that the contribution to the dijet cross section from terms of second order in σ_{18}^2 is the higher twist correction. Compared to the leading large- N_c cross section, it contains extra $\int d^2\mathbf{q}_2 \mathbf{q}_2^2 f(\mathbf{q}_2)$ and extra power of $\alpha_S \sigma_0 T(\mathbf{b})$ which combine to precisely the dimensional nuclear saturation scale $Q_A^2(\mathbf{b})$, see eq. (52), so that the resulting suppression factor is

$$\frac{d\Delta\sigma_{in}^{(1)}}{d\sigma_{in}} \sim \frac{1}{(N_c^2 - 1)} \cdot \frac{Q_A^2(\mathbf{b})}{\mathbf{p}_-^2}. \quad (71)$$

As far as an expansion in higher inverse powers of the hard scale \mathbf{p}_-^2 is concerned, $\Delta\sigma_{in}^{(1)}$ has a form of higher twist correction. In the retrospect, one observes that the principal approximation (68) in the above derivation for hard dijets amounts to putting $|\mathbf{r}|, |\mathbf{r}'| \ll |\mathbf{s}|$ in the attenuation factors in the β, β_1 integrand in (62). However, the exact \mathbf{r}, \mathbf{r}' dependence must be retained in the prefactor $\Sigma_{18}(\mathbf{s}, \mathbf{r}, \mathbf{r}')$, because it vanishes if either $\mathbf{r} = 0$ or $\mathbf{r}' = 0$. It is precisely the latter property which provides the finite difference structure of the combination of the photon wave functions in (67), (68) and is behind the higher twist property (71) of the $1/(N_c^2 - 1)$ correction.

The second term (63) gives the correction

$$\begin{aligned} & \frac{d\Delta\sigma_{in}^{(2)}}{d^2\mathbf{b}d\mathbf{z}d\mathbf{p}_-d\boldsymbol{\Delta}} = \frac{\alpha_S^3 \sigma_0^3 T^3(\mathbf{b})}{8(2\pi)^2(N_c^2 - 1)} \int_0^1 d\beta \int_0^\beta d\beta_1 \int_0^{\beta_1} d\beta_2 \\ & \times \int d^2\mathbf{q}_1 d^2\mathbf{q}_2 d^2\mathbf{q}_3 d^2\boldsymbol{\kappa}_3 f(\mathbf{q}_1) f(\mathbf{q}_2) f(\mathbf{q}_3) \\ & \times \Phi((1 - \beta + \beta_1 - \beta_2)\nu_A(\mathbf{b}), \boldsymbol{\Delta} - \boldsymbol{\kappa}_3 - \mathbf{q}_1 - \mathbf{q}_2 - \mathbf{q}_3) \Phi((1 - \beta + \beta_1 - \beta_2)\nu_A(\mathbf{b}), \boldsymbol{\kappa}_3) \\ & \times \left| \int d^2\boldsymbol{\kappa}_1 \Phi((\beta - \beta_1 + \beta_2)\nu_A(\mathbf{b}), \boldsymbol{\kappa}_1) \right. \\ & \times \left\{ \langle \gamma^* | z, \mathbf{p}_- + \boldsymbol{\kappa}_1 + \boldsymbol{\kappa}_3 \rangle - \langle \gamma^* | z, \mathbf{p}_- + \boldsymbol{\kappa}_1 + \boldsymbol{\kappa}_3 + \mathbf{q}_1 \rangle \right. \\ & - \langle \gamma^* | z, \mathbf{p}_- + \boldsymbol{\kappa}_1 + \boldsymbol{\kappa}_3 + \mathbf{q}_2 \rangle + \langle \gamma^* | z, \mathbf{p}_- + \boldsymbol{\kappa}_1 + \boldsymbol{\kappa}_3 + \mathbf{q}_1 + \mathbf{q}_2 \rangle \\ & - \langle \gamma^* | z, \mathbf{p}_- + \boldsymbol{\kappa}_1 + \boldsymbol{\kappa}_3 + \mathbf{q}_3 \rangle + \langle \gamma^* | z, \mathbf{p}_- + \boldsymbol{\kappa}_1 + \boldsymbol{\kappa}_3 + \mathbf{q}_3 + \mathbf{q}_1 \rangle \\ & \left. \left. + \langle \gamma^* | z, \mathbf{p}_- + \boldsymbol{\kappa}_1 + \boldsymbol{\kappa}_3 + \mathbf{q}_3 + \mathbf{q}_2 \rangle - \langle \gamma^* | z, \mathbf{p}_- + \boldsymbol{\kappa}_1 + \boldsymbol{\kappa}_3 + \mathbf{q}_1 + \mathbf{q}_2 + \mathbf{q}_3 | \gamma^* \rangle \right\} \right|^2. \end{aligned} \quad (72)$$

The combination of the photon wave functions in (72) corresponds to the third finite derivative in $\mathbf{q}_{1,2,3}$. Starting from (72) one can readily repeat the analysis which lead to an estimate (71). Alternatively, one can take the simplified form of the attenuation factors, as explained below eq. (71). Either way we find that contribution from third order terms in σ_{18} is of still higher twist and has a smallness

$$\frac{d\Delta\sigma_{in}^{(2)}}{d\sigma_{in}} \sim \frac{1}{(N_c^2 - 1)} \left(\frac{Q_A^2(\mathbf{b})}{\mathbf{p}_-^2} \right)^2. \quad (73)$$

Apart from the slight difference in the structure of the β integrations, the correction (64) is not any different from $d\Delta\sigma^{(1)}$ of eq. (68):

$$\begin{aligned} & \frac{d\Delta\sigma_{in}^{(3)}}{d^2\mathbf{b}dzd\mathbf{p}_-d\mathbf{\Delta}} = -\frac{\alpha_S^2\sigma_0^2T^2(\mathbf{b})}{4(2\pi)^2(N_c^2 - 1)} \int_0^1 d\beta(1 - \beta) \\ & \times \int d^2\mathbf{q}_1d^2\mathbf{q}_2d^2\boldsymbol{\kappa}_3f(\mathbf{q}_1)f(\mathbf{q}_2) \\ & \times \Phi((1 - \beta)\lambda_c\nu_A(\mathbf{b}), \mathbf{\Delta} - \boldsymbol{\kappa}_3 - \mathbf{q}_1 - \mathbf{q}_2)\Phi((1 - \beta)\lambda_c\nu_A(\mathbf{b}), \boldsymbol{\kappa}_3) \\ & \times \left| \int d^2\boldsymbol{\kappa}_1\Phi(\beta)\nu_A(\mathbf{b}), \boldsymbol{\kappa}_1 \right. \\ & \times \left. \left\{ \langle \gamma^*|z, \mathbf{p}_- + \boldsymbol{\kappa}_1 + \boldsymbol{\kappa}_3 \rangle - \langle \gamma^*|z, \mathbf{p}_- + \boldsymbol{\kappa}_1 + \boldsymbol{\kappa}_3 + \mathbf{q}_1 \rangle \right. \right. \\ & \left. \left. - \langle \gamma^*|z, \mathbf{p}_- + \boldsymbol{\kappa}_1 + \boldsymbol{\kappa}_3 + \mathbf{q}_2 \rangle + \langle \gamma^*|z, \mathbf{p}_- + \boldsymbol{\kappa}_1 + \boldsymbol{\kappa}_3 + \mathbf{q}_1 + \mathbf{q}_2 \rangle \right\} \right|^2. \quad (74) \end{aligned}$$

Consequently the same estimate (71) holds also for $d\Delta\sigma^{(3)}$.

The correction $d\Delta\sigma^{(4)}$ needs a bit more scrutiny. It contains a product of the first and second finite derivatives of the photon wave function,

$$\begin{aligned} & \frac{d\Delta\sigma_{in}^{(4)}}{d^2\mathbf{b}dzd\mathbf{p}_-d\mathbf{\Delta}} = \frac{\alpha_S^2\sigma_0^2T^2(\mathbf{b})}{2(2\pi)^2(N_c^2 - 1)} \int_0^1 d\beta(1 - \beta) \\ & \times \int d^2\mathbf{q}_1d^2\mathbf{q}_2d^2\boldsymbol{\kappa}_1d^2\boldsymbol{\kappa}_2d^2\boldsymbol{\kappa}_3f(\mathbf{q}_1)f(\mathbf{q}_2)\Phi(\beta)\nu_A(\mathbf{b}), \boldsymbol{\kappa}_1)\Phi(\beta)\nu_A(\mathbf{b}), \boldsymbol{\kappa}_2) \\ & \times \Phi((1 - \beta)\lambda_c\nu_A(\mathbf{b}), \mathbf{\Delta} - \boldsymbol{\kappa}_3 - \mathbf{q}_1 - \mathbf{q}_2)\Phi((1 - \beta)\lambda_c\nu_A(\mathbf{b}), \boldsymbol{\kappa}_3) \\ & \times \left\{ \langle \gamma^*|z, \gamma^*|z, \mathbf{p}_- + \boldsymbol{\kappa}_1 + \boldsymbol{\kappa}_3 \rangle - \langle \gamma^*|z, \gamma^*|z, \mathbf{p}_- + \boldsymbol{\kappa}_1 + \boldsymbol{\kappa}_3 + \mathbf{q}_1 \rangle \right\} \\ & \times \left\{ \langle \gamma^*|z, \mathbf{p}_- + \boldsymbol{\kappa}_1 + \boldsymbol{\kappa}_3 \rangle - \langle \gamma^*|z, \mathbf{p}_- + \boldsymbol{\kappa}_1 + \boldsymbol{\kappa}_3 + \mathbf{q}_1 \rangle \right. \\ & \left. - \langle \gamma^*|z, \mathbf{p}_- + \boldsymbol{\kappa}_1 + \boldsymbol{\kappa}_3 + \mathbf{q}_2 \rangle + \langle \gamma^*|z, \mathbf{p}_- + \boldsymbol{\kappa}_1 + \boldsymbol{\kappa}_3 + \mathbf{q}_1 + \mathbf{q}_2 \rangle \right\}, \quad (75) \end{aligned}$$

and in the interesting case of hard dijets

$$\begin{aligned} & \frac{d\Delta\sigma_{in}^{(4)}}{d^2\mathbf{b}dzd\mathbf{p}_-d\mathbf{\Delta}} = \frac{\alpha_S^2\sigma_0^2T^2(\mathbf{b})}{2(2\pi)^2(N_c^2 - 1)} \int_0^1 d\beta(1 - \beta) \\ & \times \int d^2\mathbf{q}_1d^2\mathbf{q}_2f(\mathbf{q}_1)f(\mathbf{q}_2)\Phi(2(1 - \beta)\lambda_c\nu_A(\mathbf{b}), \mathbf{\Delta} - \mathbf{q}_1 - \mathbf{q}_2) \\ & \times \left\{ \langle \gamma^*|z, \gamma^*|z, \mathbf{p}_- \rangle - \langle \gamma^*|z, \gamma^*|z, \mathbf{p}_- + \mathbf{q}_1 \rangle \right\} \\ & \times \left\{ \langle \gamma^*|z, \mathbf{p}_- \rangle - \langle \gamma^*|z, \mathbf{p}_- + \mathbf{q}_1 \rangle - \langle \gamma^*|z, \mathbf{p}_- + \mathbf{q}_2 \rangle + \langle \gamma^*|z, \mathbf{p}_- + \mathbf{q}_1 + \mathbf{q}_2 \rangle \right\}. \quad (76) \end{aligned}$$

The leading term of the small- $\mathbf{q}_{1,2}$ expansion of the product of the photon wave functions in (74) is a quadratic function of \mathbf{q}_1 and linear function of \mathbf{q}_2 of the form

$$|\langle \gamma^* | z, \mathbf{p}_- \rangle|^2 \frac{(\mathbf{p}_- \mathbf{q}_1)^2 (\mathbf{p}_- \mathbf{q}_2)}{p_-^6}. \quad (77)$$

The leading nonvanishing term comes from an expansion of the nuclear WW glue

$$\begin{aligned} & \Phi(2(1 - \beta)\lambda_c \nu_A(\mathbf{b}), \mathbf{\Delta} - \mathbf{q}_1 - \mathbf{q}_2) - \Phi(2(1 - \beta)\lambda_c \nu_A(\mathbf{b}), \mathbf{\Delta}) \\ & \sim \Phi(2(1 - \beta)\lambda_c \nu_A(\mathbf{b}), \mathbf{\Delta}) \frac{(\mathbf{\Delta}, \mathbf{q}_1 + \mathbf{q}_2)}{(2(1 - \beta)\lambda_c Q_A^2(\mathbf{b}) + \mathbf{\Delta}^2)}. \end{aligned} \quad (78)$$

Namely, upon the azimuthal averaging of (77) in conjunction with (78) we find the leading nonvanishing term of the form $2(\mathbf{p}_- \mathbf{q}_2)(\mathbf{\Delta} \mathbf{q}_2) \implies (\mathbf{p}_- \mathbf{\Delta}) \mathbf{q}_2^2$, so that

$$\frac{d\Delta\sigma_{in}^{(4)}}{d\sigma_{in}} \sim \frac{1}{(N_c^2 - 1)} \frac{(\mathbf{p}_- \mathbf{\Delta})}{\mathbf{p}_-^2}, \quad (79)$$

which is reminiscent of higher twist-3 correction.

To summarize, nonlinear nuclear k_\perp -factorization allows a consistent evaluation of $1/N_c^2$ corrections. We demonstrated how the expansion in $1/(N_c^2 - 1)$ comes along with a higher twist expansion. One exception is the reabsorption of one of the terms $\propto 1/(N_c^2 - 1)$ in σ_{88} into the renormalization of the leading term in σ_{88} by the N_c dependent factor λ_c . We conclude this discussion by a comment that all the arguments of section 5 on disappearance of azimuthal correlations of minijets hold for the $1/N_c^2$ corrections as well.

Summary and conclusions

We formulated the theory of the breakup of photons into dijets in DIS off nuclear targets based on the consistent treatment of propagation of color dipoles in nuclear medium. The non-Abelian intranuclear evolution of color dipoles gives rise to a nontrivial spectrum of the attenuation eigenvalues, still the familiar Glauber-Gribov multiple-scattering results are recovered for the nuclear total cross sections. However, for the more special cases like inelastic DIS in which the photon breaks up into the color singlet dijets, the cross section depends on the complete spectrum of the attenuation eigenstates.

We derived the nuclear broadening of acoplanarity momentum distribution in the breakup of photons into dijets, see eqs. (35), (41). Our principal finding is that all nuclear DIS observables - the amplitude of coherent diffractive breakup into dijets [6], nuclear sea quark SF and its decomposition into equally important genuine inelastic and diffractive components as carried out in [5] and the jet-jet inclusive cross section derived in the present paper, - are uniquely calculable in terms of the NSS-defined collective nuclear WW glue. This property can be regarded as a nuclear k_\perp -factorization theorem which connects DIS in the regimes of low and high density of partons. For the generic dijet cross section nuclear k_\perp -factorization is of highly nonlinear form which must be contrasted to

the linear hard factorization for the free nucleon target. This result is derived to the leading order in large- N_c , the further evaluation of the $1/N_c^2$ corrections shows a close relation between the $1/N_c^2$ and high-twist expansions. Furthermore, the $1/N_c^2$ corrections do themselves admit the nonlinear nuclear k_\perp -factorization representation.

We demonstrated a disappearance of azimuthal jet-jet correlations of minijets with momenta below the saturation scale. Based on the ideas [17, 18] on generalization of the dipole picture to hadron-nucleus collisions we presented qualitative estimates of the broadening effect for mid-rapidity jets produced in central nucleus-nucleus collisions and argued that our azimuthal decorrelation may contribute substantially to a disappearance of back-to-back high p_\perp hadron correlation in central gold-gold collisions as observed by the STAR collaboration at RHIC [20].

We conclude by the comment that all the results for hard single-jet and jet-jet inclusive cross sections can be readily extended from DIS to the breakup of projectile hadrons into forward jets. Indeed, as argued in [6], the final state interaction between the final state quark and antiquark can be neglected and plane-wave approximation becomes applicable as soon as the invariant mass of the forward jet system exceeds a typical mass scale of prominent meson and baryon resonances. The results will be presented elsewhere [36], here we confine ourselves to the statement that although our principal point about nonlinear nuclear k_\perp factorization is fully retained, we find important distinctions between the breakup of pointlike photons and non-pointlike hadrons

This work has been partly supported by the INTAS grants 97-30494 & 00-00366 and the DFG grant 436RUS17/119/02

Appendix A: Calculation of the 4-body color dipole cross section

The Feynman diagrams for the matrix of 4-parton dipole cross section $\sigma_4(\mathbf{s}, \mathbf{r}, \mathbf{r}')$, eqs. (19)-(21) are shown in fig. 2. The profile function for the color-singlet $q\bar{q}$ pair is given by the diagrams of fig. 2a-2c:

$$2\Gamma(\text{fig.2a} - 2c; (q\bar{q})_1 N; \mathbf{b}_+, \mathbf{b}_-) = \frac{1}{N_c} \delta_{ab} \{ [\chi^2(\mathbf{b}_+) + \chi^2(\mathbf{b}_-)] \text{Tr}(T^a T^b) - 2\chi(\mathbf{b}_+)\chi(\mathbf{b}_-) \text{Tr}(T^a T^b) \} = \frac{N_c^2 - 1}{2N_c} [\chi(\mathbf{b}_+) - \chi(\mathbf{b}_-)]^2, \quad (80)$$

which has already been cited in the main text, eq. (11). Upon adding the contribution from diagrams of fig. 2e-2h, we obtain an obvious result (19).

The color-diagonal contribution of the same diagrams to the interaction of the color-octet $q\bar{q}$ pair with the nucleon equals

$$2\Gamma(\text{fig.2a} - 2c; (q\bar{q})_8 N; \mathbf{b}_+, \mathbf{b}_-) = \frac{2}{N_c^2 - 1} \delta_{ab} \{ [\chi^2(\mathbf{b}_+) + \chi^2(\mathbf{b}_-)] \text{Tr}(T^c T^a T^b T^c) - 2\chi(\mathbf{b}_+)\chi(\mathbf{b}_-) \text{Tr}(T^c T^a T^c T^b) \} = \frac{N_c^2 - 1}{2N_c} \left\{ [\chi^2(\mathbf{b}_+) + \chi^2(\mathbf{b}_-)] + \frac{2}{N_c^2 - 1} \chi(\mathbf{b}_+)\chi(\mathbf{b}_-) \right\}. \quad (81)$$

A contribution to the matrix element $\langle 88 | \sigma_4 | 88 \rangle$ from color-diagonal interactions of the $(q'\bar{q}')$ pair is obtained from (82) by the substitution $\mathbf{b}_\pm \rightarrow \mathbf{b}'_\pm$:

$$\Gamma_4(\text{fig.2a} - 2c + \text{fig.2e} - 2h; (88)N; \mathbf{b}_+, \mathbf{b}_-, \mathbf{b}'_+, \mathbf{b}'_-) = \Gamma(\text{fig.2a} - 2c; q\bar{q})_8 N; \mathbf{b}_+, \mathbf{b}_-) + \Gamma(\text{fig.2a} - 2c; q\bar{q})_8 N; \mathbf{b}'_+, \mathbf{b}'_-). \quad (82)$$

The diagrams of fig. 2e-2h describe processes with color-space rotation of the $(q\bar{q})$ pair:

$$2\Gamma_4(\text{fig.2i} - 2l; (88)N \rightarrow (88)N; \mathbf{b}_+, \mathbf{b}_-, \mathbf{b}'_+, \mathbf{b}'_-) = \frac{8}{N_c^2 - 1} \delta_{ab} \left\{ [\chi(\mathbf{b}_+)\chi(\mathbf{b}'_-) + \chi(\mathbf{b}_-)\chi(\mathbf{b}'_+)] \text{Tr}(T^c T^a T^d) \text{Tr}(T^c T^b T^d) - [\chi(\mathbf{b}_+)\chi(\mathbf{b}'_+) + \chi(\mathbf{b}_-)\chi(\mathbf{b}'_-)] \text{Tr}(T^c T^a T^d) \text{Tr}(T^d T^b T^c) \right\} = -\frac{N_c^2 - 1}{N_c} \left\{ \frac{2}{N_c^2 - 1} [\chi(\mathbf{b}_+)\chi(\mathbf{b}'_-) + \chi(\mathbf{b}_-)\chi(\mathbf{b}'_+)] + \frac{N_c^2 - 2}{N_c^2 - 1} [\chi(\mathbf{b}_+)\chi(\mathbf{b}'_+) + \chi(\mathbf{b}_-)\chi(\mathbf{b}'_-)] \right\}. \quad (83)$$

The $(11)N \rightarrow (88)N$ transition matrix element comes from diagrams of fig. 2e-h:

$$\begin{aligned}
& 2\Gamma_4(2i-l; (11)N \rightarrow (88)N; \mathbf{b}_+, \mathbf{b}_-, \mathbf{b}'_+, \mathbf{b}'_-) = \\
& \frac{4}{N_c \sqrt{N_c^2 - 1}} \delta_{ab} \left\{ \left[\chi(\mathbf{b}_+) \chi(\mathbf{b}'_-) + \chi(\mathbf{b}_-) \chi(\mathbf{b}'_+) \right] \text{Tr}(T^c T^a) \text{Tr}(T^c T^b) \right. \\
& \left. - \left[\chi(\mathbf{b}_+) \chi(\mathbf{b}'_+) + \chi(\mathbf{b}_-) \chi(\mathbf{b}'_-) \right] \text{Tr}(T^c T^a) \text{Tr}(T^c T^b) \right\} \\
& = \frac{N_c^2 - 1}{N_c} \cdot \frac{1}{\sqrt{N_c^2 - 1}} \left\{ \left[\chi(\mathbf{b}_+) \chi(\mathbf{b}'_-) + \chi(\mathbf{b}_-) \chi(\mathbf{b}'_+) \right] \right. \\
& \left. - \left[\chi(\mathbf{b}_+) \chi(\mathbf{b}'_+) + \chi(\mathbf{b}_-) \chi(\mathbf{b}'_-) \right] \right\}. \tag{84}
\end{aligned}$$

Upon the rearrangement $-2\chi(\mathbf{b}_i)\chi(\mathbf{b}_j) = [\chi(\mathbf{b}_i) - \chi(\mathbf{b}_j)]^2 - \chi^2(\mathbf{b}_i) - \chi^2(\mathbf{b}_j)$ one can readily verify that the terms $\propto \chi^2(\mathbf{b}_i)$ cancel each other, and the 4-body cross section will be a linear combination of $\sigma(\mathbf{b}_i - \mathbf{b}_j)$, recall a discussion in [24].

Appendix B: Non-Abelian vs. Abelian aspects of intranuclear propagation of color dipoles and Glauber-Gribov formalism

The intranuclear propagation of color-octet $q\bar{q}$ pairs is part and parcel of a complete formalism for DIS off nucleus. It is interesting to see how one recovers the quasi-Abelian color-dipole results for the nuclear cross sections [13, 14] which are of the Glauber-Gribov form [21, 22]. We consider first the total inelastic cross section obtained from (8) upon the integration over the transverse momenta \mathbf{p}_\pm of the quark and antiquark, which amounts to putting $\mathbf{b}_+ = \mathbf{b}'_+$ and $\mathbf{b}_- = \mathbf{b}'_-$. Then we are left with the system of two color dipoles of the same size $\mathbf{r} = \mathbf{b}_+ - \mathbf{b}_- = \mathbf{r}' = \mathbf{b}'_+ - \mathbf{b}'_-$, and the matrix of the 4-body cross section has the eigenvalues

$$\Sigma_1 = 0, \tag{85}$$

$$\Sigma_2 = \frac{2N_c^2}{N_c^2 - 1} \sigma(\mathbf{r}) \tag{86}$$

with the eigenstates

$$|f_1\rangle = \frac{1}{N_c} (|11\rangle + \sqrt{N_c^2 - 1}|88\rangle), \tag{87}$$

$$|f_2\rangle = \frac{1}{N_c} (\sqrt{N_c^2 - 1}|11\rangle - |88\rangle). \tag{88}$$

The existence of the non-attenuating 4-quark state with $\Sigma_1 = 0$ is quite obvious and corresponds to an overlap of two $q\bar{q}$ dipoles of the same size with neutralization of color

charges. An existence of such a non-attenuating state is shared by an Abelian and non-Abelian quark-gluon interaction. The intranuclear attenuation eigen-cross section (86) differs from $\sigma(\mathbf{r})$, for the color-singlet $q\bar{q}$ pair by the nontrivial color factor $2\lambda_c = 2N_c^2/(N_c^2 - 1) = C_A/C_F$ which derives from the relevant 4-parton state being in the color octet-(anti)octet configuration.

The crucial point is that the final state which enters the calculation of the genuine inelastic DIS off a nucleus, see eq. (15), is precisely the eigenstate $|f_1\rangle$. Then, even without invoking the Sylvester expansion (23), (25), the straightforward result for the inelastic cross section is

$$\begin{aligned}\sigma_{in} &= \int d^2\mathbf{r} dz |\Psi(Q^2, z, \mathbf{r})|^2 \int d^2\mathbf{b} \left\{ N_c \langle f_1 | \exp \left[-\frac{1}{2} \sigma_4 T(\mathbf{b}) \right] |11\rangle - \exp [-\sigma(\mathbf{r})T(\mathbf{b})] \right\} \\ &= \int d^2\mathbf{b} \langle \gamma^* | \left\{ \exp \left[-\frac{1}{2} \Sigma_1 T(\mathbf{b}) \right] - \exp [-\sigma(\mathbf{r})T(\mathbf{b})] \right\} | \gamma^* \rangle \\ &= \int d^2\mathbf{b} \langle \gamma^* | \{ 1 - \exp [-\sigma(\mathbf{r})T(\mathbf{b})] \} | \gamma^* \rangle\end{aligned}\quad (89)$$

what is precisely the color-dipole generalization [14] of the Glauber-Gribov formula [21, 22] in which no trace of a non-Abelian intranuclear evolution with the nontrivial attenuation eigenstate (88) with the eigen-cross section (86) is left.

When the photon breaks into the color-singlet $q\bar{q}$ dijet, the net flow of color between the $q\bar{q}$ pair and color-excited debris of the target nucleus is zero. Which suggests that a rapidity gap may survive upon the hadronization, although whether a rapidity gap in genuine inelastic events with color-singlet $q\bar{q}$ production is stable against higher order correction or not remains an interesting open issue. Although the debris of the target nucleus have a zero net color charge, the debris of color-excited nucleons are spatially separated by a distance of the order of the nuclear radius, which suggests a total excitation energy of the order of 1 GeV times $A^{1/3}$, so that such a rapidity-gap events would look like a double diffraction with multiple production of mesons in the nucleus fragmentation region (for the theoretical discussion of conventional mechanisms of diffraction excitation of nuclei in proton-nucleus collisions see [37], the experimental observation has been reported in [38]). As such, inelastic excitation of color-singlet dijets is distinguishable from quasielastic diffractive DIS followed by excitation and breakup of the target nucleus without production of secondary particles.

Making use of the Sylvester expansion (23)-(25), and the eigenstates (87),(88), one readily obtains

$$\begin{aligned}\sigma_{in}(A^*(q\bar{q})_1) &= \int d^2\mathbf{b} \\ &\times \langle \gamma^* | \left\{ (1 - \exp [-\sigma(\mathbf{r})T(\mathbf{b})]) - \frac{N_c^2 - 1}{N_c^2} (1 - \exp \left[-\frac{1}{2} \Sigma_2 T(\mathbf{b}) \right]) \right\} | \gamma^* \rangle,\end{aligned}\quad (90)$$

$$\sigma_{in}(A^*(q\bar{q})_8) = \frac{N_c^2 - 1}{N_c^2} \int d^2\mathbf{b} \langle \gamma^* | \left\{ 1 - \exp \left[-\frac{1}{2} \Sigma_2 T(\mathbf{b}) \right] \right\} | \gamma^* \rangle.\quad (91)$$

which depend on the whole non-Abelian spectrum of attenuation eigenstates.

Several features of the result (90) are noteworthy. First, the color neutralization of the $q\bar{q}$ pair after the first inelastic interaction requires at least one more secondary inelastic interaction, and an expansion of the integrand of $\sigma_{in}(A^*(q\bar{q})_1)$ starts with the term quadratic in the optical thickness:

$$\left\{ (1 - \exp[-\sigma(\mathbf{r})T(\mathbf{b})]) - \frac{N_c^2 - 1}{N_c^2} (1 - \exp[-\frac{1}{2}\Sigma_2 T(\mathbf{b})]) \right\} = \frac{1}{2(N_c^2 - 1)} \sigma^2(\mathbf{r}) T^2(\mathbf{b}) + \dots (92)$$

Second, in the large- N_c limit the color octet state tends to oscillate in color remaining in the octet state. This is clearly seen from (92). Third, in the limit of an opaque nucleus

$$\sigma_{in}(A^*(q\bar{q})_1) = \frac{1}{N_c^2} \int d^2\mathbf{b} \langle \gamma^* | \{1 - \exp[-\sigma(\mathbf{r})T(\mathbf{b})]\} | \gamma^* \rangle = \frac{1}{N_c^2} \sigma_{in} \quad (93)$$

and remains a constant fraction of DIS in contrast to the quasielastic diffractive DIS or inelastic diffractive excitation of a nucleus, the cross sections of which vanish for an opaque nucleus [14, 37].

An analysis of the single-parton, alias the single-jet, inclusive cross section is quite similar. In this case we integrate over the momentum \mathbf{p}_- of the antiquark jet, so that $\mathbf{b}'_- = \mathbf{b}_-$. The corresponding matrix σ_4 has the eigenvalues

$$\Sigma_1 = \sigma(\mathbf{r} - \mathbf{r}') \quad (94)$$

$$\Sigma_2 = \frac{N_c^2}{N_c^2 - 1} [\sigma(\mathbf{r}) + \sigma(\mathbf{r}')] - \frac{1}{N_c^2 - 1} \sigma(\mathbf{r} - \mathbf{r}') \quad (95)$$

with exactly the same eigenstates $|f_1\rangle$ and $|f_2\rangle$ as given by eqs. (87),(88). Again, the cross section of genuine inelastic DIS corresponds to projection onto the eigenstate $|f_1\rangle$, so that

$$\begin{aligned} \frac{d\sigma_{in}}{d^2\mathbf{b}d^2\mathbf{p}dz} &= \frac{1}{(2\pi)^2} \int d^2\mathbf{r}' d^2\mathbf{r} \exp[i\mathbf{p}(\mathbf{r}' - \mathbf{r})] \Psi^*(Q^2, z, \mathbf{r}') \Psi(Q^2, z, \mathbf{r}) \\ &\times \left\{ \exp[-\frac{1}{2}\Sigma_1 T(\mathbf{b})] - \exp[-\frac{1}{2}[\sigma(\mathbf{r}) + \sigma(\mathbf{r}')T(\mathbf{b})]] \right\} \\ &= \frac{1}{(2\pi)^2} \int d^2\mathbf{r}' d^2\mathbf{r} \exp[i\mathbf{p}(\mathbf{r}' - \mathbf{r})] \Psi^*(Q^2, z, \mathbf{r}') \Psi(Q^2, z, \mathbf{r}) \\ &\times \left\{ \exp[-\frac{1}{2}\sigma(\mathbf{r} - \mathbf{r}')T(\mathbf{b})] - \exp[-\frac{1}{2}[\sigma(\mathbf{r}) + \sigma(\mathbf{r}')T(\mathbf{b})]] \right\}. \quad (96) \end{aligned}$$

which is precisely an eq. (10) of ref. [5].

At this point we emphasize that for the fundamental reason that the relevant final state is precisely the eigenstate $|f_1\rangle$, the calculation of the integrated inelastic cross section (89), as well as the one-particle inclusive inelastic spectrum (96), are both essentially Abelian problems, and the final result (96) is identical, apart from the very different notations, to that derived by one of the authors (BGZ) for the propagation of relativistic positronium in dense media [32]. As one could see from an inspection of the

relevant four-parton states, all contributions from the propagation of color-octet dipoles cancel out, and the results could have been obtained from studying the propagation of color-singlet dipoles without any reference to the full cross section matrix σ_4 . Our formalism makes these cancellations nicely explicit. These quasi-Abelian problems have been studied also in [2, 40].

Appendix C: Weizsäcker-Williams glue of spatially overlapping nucleons

According to [5, 6] the multiple convolutions $f^{(j)}(\boldsymbol{\kappa})$ have a meaning of the collective unintegrated gluon SF of j nucleons at the same impact parameter the Weizsäcker-Williams gluon fields of which overlap spatially in the Lorentz contracted nucleus. These convolutions can also be viewed as a random walk in which $f(\boldsymbol{\kappa})$ describes the single walk distribution.

To the lowest order in pQCD, the large $\boldsymbol{\kappa}^2$ behavior is $f(\boldsymbol{\kappa}) \propto \alpha_S(\boldsymbol{\kappa}^2)/\boldsymbol{\kappa}^4$, the phenomenological study of the differential glue of the proton in [19] suggests a useful large- $\boldsymbol{\kappa}^2$ approximation $f(\boldsymbol{\kappa}) \propto 1/(\boldsymbol{\kappa}^2)^\gamma$ with the exponent $\gamma \sim 2$ (a closer inspection of numerical results in [19] gives $\gamma \approx 2.15$ at $x = 10^{-2}$). The QCD evolution effects enhance $f(\boldsymbol{\kappa})$ at large $\boldsymbol{\kappa}^2$, the smaller is x the stronger is an enhancement.

Because $f(\boldsymbol{\kappa})$ decreases very slowly, we encounter a manifestly non-Gaussian random walk. For instance, as was argued in [6], a j -fold walk to large $\boldsymbol{\kappa}^2$ is realized by one large walk, $\boldsymbol{\kappa}_1^2 \sim \boldsymbol{\kappa}^2$, accompanied by $(j-1)$ small walks. We simply cite here the main result [6]

$$f^{(j)}(\boldsymbol{\kappa}) = j \cdot f(\boldsymbol{\kappa}) \left[1 + \frac{4\pi^2(j-1)\gamma^2}{N_c\sigma_0\boldsymbol{\kappa}^2} \cdot G(\boldsymbol{\kappa}^2) \right], \quad (97)$$

where $G(\boldsymbol{\kappa}^2)$ is the conventional integrated gluon SF. Then the hard tail of unintegrated nuclear glue per bound nucleon, $f_{WW}(\mathbf{b}, \boldsymbol{\kappa}) = \phi_{WW}(\nu_A(\mathbf{b}), \boldsymbol{\kappa})/\nu_A(\mathbf{b})$, can be calculated parameter free:

$$\begin{aligned} f_{WW}(\mathbf{b}, \boldsymbol{\kappa}) &= \frac{1}{\nu_A(\mathbf{b})} \cdot \sum_{j=1}^{\infty} w_j(\nu_A(\mathbf{b})) j f^{(j)}(\boldsymbol{\kappa}) \left[1 + \frac{4\pi^2\gamma^2}{N_c\sigma_0\boldsymbol{\kappa}^2} \cdot (j-1)G(\boldsymbol{\kappa}^2) \right] \\ &= f(\boldsymbol{\kappa}) \left[1 + \frac{2C_A\pi^2\gamma^2\alpha_S(r)T(\mathbf{b})}{C_F N_c \boldsymbol{\kappa}^2} G(\boldsymbol{\kappa}^2) \right]. \end{aligned} \quad (98)$$

In the hard regime the differential nuclear glue is not shadowed, furthermore, because of the manifestly positive-valued and model-independent nuclear higher twist correction it exhibits a nuclear antishadowing property [6].

Now we present the arguments in favor of the scaling small- $\boldsymbol{\kappa}$ behavior

$$f^{(j)}(\boldsymbol{\kappa}^2) \approx \frac{1}{Q_j^2} \xi\left(\frac{\boldsymbol{\kappa}^2}{Q_j^2}\right) \approx \frac{1}{\pi} \frac{Q_j^2}{(\boldsymbol{\kappa}^2 + Q_j^2)^2} \quad (99)$$

with

$$Q_j^2 \approx jQ_0^2. \quad (100)$$

In an evolution of $f^{(j)}(\boldsymbol{\kappa})$ with j at moderate $\boldsymbol{\kappa}^2$,

$$f^{(j+1)}(\boldsymbol{\kappa}^2) = \int d^2\mathbf{k} f(\mathbf{k}^2) f^{(j)}((\boldsymbol{\kappa} - \mathbf{k})^2), \quad (101)$$

the function $f(\mathbf{k}^2)$ is a steep one compared to a smooth and broad $f^{(j)}((\boldsymbol{\kappa} - \mathbf{k})^2)$, so that we can expand

$$\begin{aligned} f^{(j)}((\boldsymbol{\kappa} - \mathbf{k})^2) &= f^{(j)}(\boldsymbol{\kappa}^2) + \frac{df^{(j)}(\boldsymbol{\kappa}^2)}{d\boldsymbol{\kappa}^2} [\mathbf{k}^2 - 2\boldsymbol{\kappa}\mathbf{k}] + \frac{1}{2} \frac{d^2f^{(j)}(\boldsymbol{\kappa}^2)}{(d\boldsymbol{\kappa}^2)^2} 4(\boldsymbol{\kappa}\mathbf{k})^2 \\ \implies f^{(j)}(\boldsymbol{\kappa}^2) + \mathbf{k}^2 \left[\frac{df^{(j)}(\boldsymbol{\kappa}^2)}{d\boldsymbol{\kappa}^2} + \boldsymbol{\kappa}^2 \frac{d^2f^{(j)}(\boldsymbol{\kappa}^2)}{(d\boldsymbol{\kappa}^2)^2} \right] &= f^{(j)}(\boldsymbol{\kappa}^2) + \mathbf{k}^2 \frac{d}{d\boldsymbol{\kappa}^2} \left[\boldsymbol{\kappa}^2 \frac{df^{(j)}(\boldsymbol{\kappa}^2)}{d\boldsymbol{\kappa}^2} \right]. \end{aligned} \quad (102)$$

Here \implies indicates an azimuthal averaging. The expansion (102) holds for $\boldsymbol{\kappa}^2 \lesssim Q_j^2$ and upon the $d^2\mathbf{k}$ integration in (101) we obtain

$$f^{(j+1)}(\boldsymbol{\kappa}^2) = f^{(j)}(\boldsymbol{\kappa}^2) + g(j) \frac{d}{d\boldsymbol{\kappa}^2} \left[\boldsymbol{\kappa}^2 \frac{df^{(j)}(\boldsymbol{\kappa}^2)}{d\boldsymbol{\kappa}^2} \right], \quad (103)$$

where

$$g(j) = \int^{Q_j^2} d^2\mathbf{k} \mathbf{k}^2 f(\mathbf{k}^2) = \frac{4\pi^2}{N_c \sigma_0} G(Q_j^2). \quad (104)$$

It is a smooth function of j . One can readily check that our approximation preserves the normalization condition $\int d^2\boldsymbol{\kappa} f^{(j)}(\boldsymbol{\kappa}) = 1$.

For small $\boldsymbol{\kappa}^2$ and large j the recurrence relation (104) amounts to the differential equation

$$\frac{Q_{j+1}^2 - Q_j^2}{Q_{j+1}^2 Q_j^2} = \frac{1}{Q_j^4} \cdot \frac{dQ_j^2}{dj} = -\frac{1}{Q_j^4} \frac{\xi'(0)}{\xi(0)} g(j) \quad (105)$$

with the solution

$$Q_j^2 = -\frac{\xi'(0)}{\xi(0)} \int^j dj' g(j') \approx -j g(j) \frac{\xi'(0)}{\xi(0)} \quad (106)$$

The expansion (102) holds up to the terms $\propto \boldsymbol{\kappa}^2$ and its differentiation at $\boldsymbol{\kappa}^2 = 0$ gives a similar constraint on the j -dependence of Q_j^2 .

We notice that the expansion of the plateau with j entails a dilution of the differential collective glue $f^{(j)}(\boldsymbol{\kappa}^2)$ in the plateau region, $f^{(j)}(\boldsymbol{\kappa}^2 \lesssim Q_j^2) \propto 1/Q_j^2 \propto 1/j$. We conclude by the observation that when extended to $\boldsymbol{\kappa}^2 \gtrsim Q_j^2$, the parameterization (101), (100) has the behavior $jQ_0^2/(\boldsymbol{\kappa}^2)^2$ which nicely matches the j -dependence of the leading twist term in the hard asymptotics (99).

For a heavy nucleus the dominant contribution to the expansion (31) comes from $j \approx \nu_A(\mathbf{b})$, so that

$$\phi_{WW}(\nu_A(\mathbf{b}), \boldsymbol{\kappa}) \approx \frac{1}{\pi} \frac{Q_A^2(\mathbf{b})}{(\boldsymbol{\kappa}^2 + Q_A^2(\mathbf{b}))^2}, \quad (107)$$

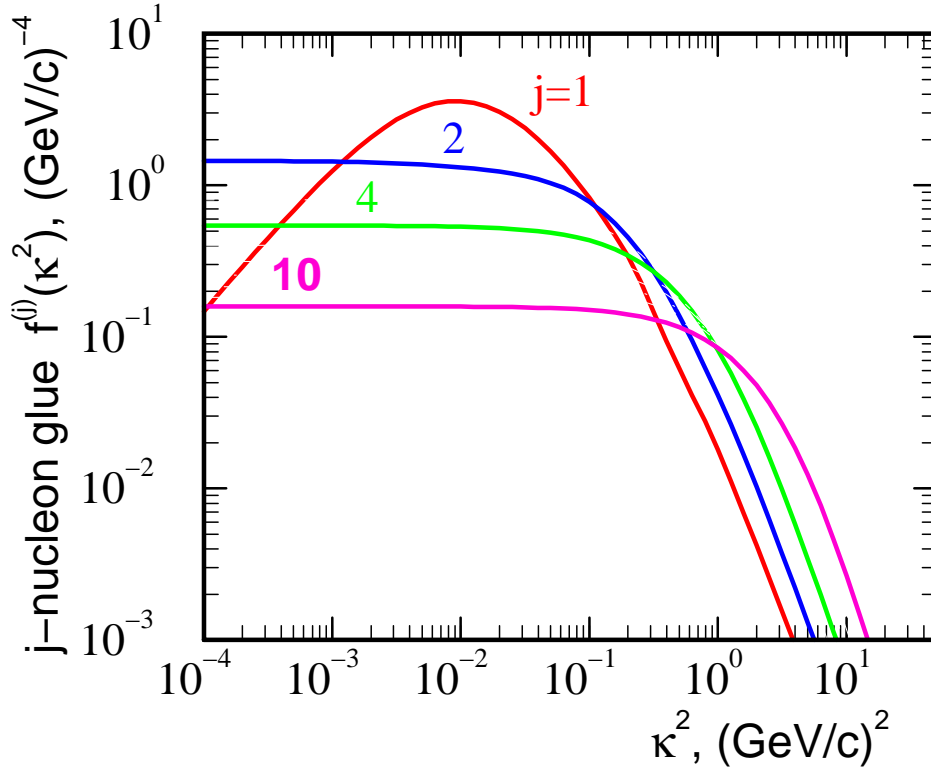


Figure 7: *The nuclear dilution for soft momenta and broadening for hard momenta of the collective glue of j overlapping nucleons $f^{(j)}(\boldsymbol{\kappa})$. The numerical results are for DIS at $x = 0.01$ and the input unintegrated gluon SF of the proton is taken from ref. [19]*

where (106) gives the width of the plateau

$$Q_A^2(\mathbf{b}) \approx 2\nu_A(\mathbf{b})g(\nu_A(\mathbf{b})) \approx \frac{4\pi^2}{N_c}\alpha_S(Q_A^2)G(Q_A^2)T(\mathbf{b}). \quad (108)$$

The explicit dependence on the soft parameter σ_0 manifest in (104) cancels out in (108). For DIS within the saturation domain, $Q^2 \lesssim Q_A^2$, the strong coupling in (33) must be taken at $r \sim 1/Q_A$, and the r.h.s. of (108) exhibits only weak dependence on the infrared parameters through the Q_A^2 dependence of the running strong coupling and scaling violations in the gluon SF of the nucleon. For instance, at $x = 10^{-2}$ the numerical results [19] for $G(Q^2)$ correspond to a nearly Q^2 independent $\alpha_S(Q^2)G(Q^2) \approx 1$. For average DIS on a heavy nucleus

$$\langle T(\mathbf{b}) \rangle \approx \frac{3}{4}T(0) \approx \frac{9}{8\pi r_0^2}A^{1/3} \quad (109)$$

where $r_0 \approx 1.1\text{fm}$. For lighter nuclei with the Gaussian density profile $\langle T(\mathbf{b}) \rangle \approx \frac{1}{2}T(0)$. Then for $N_c = 3$ and $A^{1/3} = 6$ eqs. (108) and (109) give $\langle Q_A^2(\mathbf{b}) \rangle \approx 0.8 \text{ (GeV/c)}^2$.

The utility of an approximation (99), (100) is illustrated by fig. 7, where we show the j -dependence of the collective glue of j overlapping nucleons calculated for the un-integrated gluon SF of the proton from ref. [19]. For interaction of $q\bar{q}$ color dipoles in average DIS off the gold, ^{197}Au , target we find $\langle Q_{3A}^2(\mathbf{b}) \rangle \approx 0.9 \text{ (GeV}/c)^2$ in good agreement with the above estimate from (108). For the $q\bar{q}g$ Fock states of the photon the leading $\log Q^2$ configurations correspond to small $q\bar{q}$ pairs which act as a color-octet gluon [24] and for such gluon-gluon color dipoles $\langle Q_{8A}^2(\mathbf{b}) \rangle \approx 2.1 \text{ (GeV}/c)^2$. We note in passing that the standard collinear splitting sets in, and the DGLAP evolution [34, 41] becomes applicable to nuclear structure function, only at $Q^2 \gg \langle Q_{8A}^2(\mathbf{b}) \rangle$.

References

- [1] E. Leader and E. Predazzi, Introduction to Gauge Theories and Modern Particle Physics, v.1, Cambridge University Press, Cambridge, 1996; G. Sterman, An Introduction to Quantum Field Theory, Cambridge University Press, Cambridge, 1993.
- [2] A.H. Mueller, *Nucl. Phys.* **B558** (1999) 285; Lectures at the Cargèse Summer School, August 6-18, 2001, [arXiv:hep-ph/0111244](#).
- [3] A.H. Mueller, *Nucl. Phys.* **B335** (1990) 115.
- [4] L. McLerran and R. Venugopalan, *Phys. Rev.* **D49** (1994) 2233; **D55** (1997) 5414; E. Iancu, A. Leonidov and L. McLerran, Lectures at the Cargèse Summer School, August 6-18, 2001, [arXiv:hep-ph/0202270](#).
- [5] N.N. Nikolaev, W. Schäfer, B.G. Zakharov, V.R. Zoller. *JETP Lett.* **76** (2002) 195.
- [6] N.N. Nikolaev, W. Schäfer and G. Schwiete, *JETP Lett.* **72** (2000) 583; *Pisma Zh. Eksp. Teor. Fiz.* **72** (2000) 583; *Phys. Rev.* **D63** (2001) 014020.
- [7] L.N.Lipatov, *Sov. J. Nucl. Phys* **23** (1976) 338; E.A.Kuraev, L.N.Lipatov and V.S.Fadin, *Sov. Phys. JETP* **44** (1976) 443; *ibid.* **45** (1977) 199; Ya.Ya.Balitsky and L.N.Lipatov, *Sov. J. Nucl. Phys* **28** (1978) 822
- [8] I.P. Ivanov, N.N. Nikolaev, W. Schäfer, B.G. Zakharov and V.R. Zoller, Lectures on Diffraction and Saturation of Nuclear Partons in DIS off Heavy Nuclei, Proceedings of 36-th Annual Winter School on Nuclear and Particle Physics and 8-th St. Petersburg School on Theoretical Physics, St. Petersburg, Russia, 25 Feb - 3 Mar 2002. [arXiv: hep-ph/0212161](#)
- [9] I.P. Ivanov, N.N. Nikolaev, W. Schäfer, B.G. Zakharov and V.R. Zoller, High Density QCD, Saturation and Diffractive DIS. Invited talk at the NATO Advanced Research Workshop on Diffraction 2002, Alushta, Ukraine, 31 Aug - 6 September 2002. e-Print Archive: [hep-ph/0212176](#); Diffractive Hard Dijets and Nuclear Parton Distributions, Proceedings of the Workshop on Exclusive Processes at High Momentum Transfer, Jefferson Lab, May 15-18, 2002. Editors A. Radyushkin and P. Stoler, World Scientific, 2002, pp. 205-213; High Density QCD and Saturation of Nuclear Partons, Proceedings of the Conference on Quark Nuclear Physics (QNP'2002), June 9-14, Jülich, Germany, editors C. Elster and Th. Walcher, *Eur. Phys. J* (2003) in print, e-Print Archive: [hep-ph/0209298](#); High Density QCD, Saturation and Diffractive DIS. Plenary talk at the International Symposium on Multiparticle Dynamics (ISMD'2002), Alushta, Ukraine, 8-14 September 2002, ed. G. Kozlov and A. Sissakian, World Scientific (2003) in print.

- [10] T. Ahmed et al. (H1 Collaboration), *Nucl. Phys.* **B445**, 195 (1995) and references therein.
- [11] A. Szczurek, N.N. Nikolaev, W. Schäfer, J. Speth, *Phys. Lett.* **B500** , 254 (2001)
- [12] J. R. Forshaw and R. G. Roberts, *Phys. Lett. B* **335**, 494 (1994); A. J. Askew, D. Graudenz, J. Kwiecinski and A. D. Martin, *Phys. Lett. B* **338**, 92 (1994); J. Kwiecinski, A. D. Martin and A. M. Stasto, *Phys. Lett. B* **459**, 644 (1999);
- [13] N.N. Nikolaev and B.G. Zakharov, *Z. Phys.* **C49** (1991) 607
- [14] N.N. Nikolaev, B.G. Zakharov and V.R. Zoller, *Z. Phys.* **A351** (1995) 435.
- [15] V. Barone, M. Genovese, N.N. Nikolaev, E. Predazzi and B.G. Zakharov. *Z. Phys.* **C58** (1993) 541
- [16] N.N. Nikolaev and V.I. Zakharov, *Sov. J. Nucl. Phys.* **21** (1975) 227; [*Yad. Fiz.* **21** (1975) 434]; *Phys. Lett.* **B55** (1975) 397.
- [17] N.N. Nikolaev, G. Piller and B.G. Zakharov. *J. Exp. Theor. Phys.* **81** (1995) 851; *Z. Phys.* **A354** (1996) 99
- [18] B.G. Zakharov, *JETP Lett.* **63** (1996) 952; *JETP Lett.* **65** (1997) 615; *Phys. Atom. Nucl.* **61** (1998) 838;
- [19] I.P. Ivanov and N.N. Nikolaev, *Phys. Atom. Nucl.* **64**, 753 (2001), *Yad. Fiz.* **64**, 813 (2001); *Phys. Rev.* **D65** 054004 (2002).
- [20] C. Adler, et al. (STAR Collaboration), *Phys. Rev. Lett.* **90**, 082302 (2003)
- [21] R. J. Glauber, in *Lectures in Theoretical Physics*, edited by W. E. Brittin et al. (Interscience Publishers, Inc., New York, 1959), Vol. 1, p. 315.
- [22] V.N. Gribov, *Sov. Phys. JETP* **29** (1969) 483; *Zh. Eksp. Teor. Fiz.* **56** (1969) 892.
- [23] N.N. Nikolaev and B.G. Zakharov, *Z. Phys.* **C53** (1992) 331.
- [24] N.N. Nikolaev and B.G. Zakharov, *J. Exp. Theor. Phys.* **78** (1994) 806; [*Zh. Eksp. Teor. Fiz.* **105** (1994) 1498]; *Z. Phys.* **C64** (1994) 631.
- [25] N.N. Nikolaev, B.G. Zakharov and V.R. Zoller, *JETP Lett.* **59** (1994) 6
- [26] N.N. Nikolaev and B.G. Zakharov. *Phys. Lett.* **B332** (1994) 184
- [27] V. Barone, M. Genovese, N.N. Nikolaev, E. Predazzi and B.G. Zakharov. *Phys. Lett.* **B326** (1994) 161
- [28] B. Andersson *et al.* (Small x Collaboration), *Eur. Phys. J.* **C25**, 77 (2002)
- [29] M. Genovese, N.N. Nikolaev and B.G. Zakharov, *J. Exp. Theor. Phys.* **81** (1995) 633; *Zh. Eksp. Teor. Fiz.* **108** (1995) 1155

- [30] C. Adloff et al. (H1 Collab.), *Z. Phys.* **C76** (1997) 613
- [31] J. Breitweg et al. (ZEUS Collaboration), *Europ. Phys. J.* **C6** (1999) 43.
- [32] B.G. Zakharov, *Sov. J. Nucl. Phys.* **46** (1987) 92; *Yad. Fiz.* **46** (1987) 148.
- [33] N.N. Nikolaev, J. Speth, B.G. Zakharov, *J. Exp. Theor. Phys.* **82** (1996) 1046; *Zh. Eksp. Teor. Fiz.* **109** (1996) 1948
- [34] Yu.L. Dokshitzer, *Sov. Phys. JETP* **46** (1977) 641; *Zh. Eksp. Teor. Fiz.* **73**, 1216 (1977); Yu.L. Dokshitzer, D. Diakonov, S.I. Troian, *Phys. Rept.* **58**, 269 (1980)
- [35] T. Sjöstrand et al., *Comp. Phys. Commun.* **135** (2001) 238
- [36] N.N. Nikolaev, W. Schäfer, B.G. Zakharov and V.R. Zoller, paper in preparation.
- [37] V.R. Zoller, *Z. Phys.* **C51** (1991) 659; M.A. Faessler, *Z. Phys.* **C58** (1993) 567.
- [38] T. Akesson et al. (HELIOS Collab.), *Z. Phys.* **C49** (1991) 355
- [39] H. De Vries, C.W. De Jaeger, C. De Vries, *Atomic Data and Nuclear Data Tables* **36**, 495 (1987)
- [40] U. A. Wiedemann, *Nucl. Phys.* **B582**, 409 (2000)
- [41] V.N. Gribov and L.N. Lipatov, *Sov. J. Nucl. Phys.* **15** (1972) 438; L.N. Lipatov, *Sov. J. Nucl. Phys.* **20** (1974) 181; G. Altarelli and G. Parisi, *Nucl. Phys.* **B126** (1977) 298.